

Dear Editor,

While editing for addressing all of the reviewers comments and suggestions we found that the quality of the manuscript could have been further improved by making a series of changes. These do not imply any significant change in the overall message but they still deserved to be addressed. This is the list of changes:

- The fields RMSD and Bias in Table 5 along with \bar{X}^M , \bar{X}^E , RMSD, bias CMRSD and MAE in Table S.8 all changed because in the current version we used the log-transformation only to compute the linear fit parameters (slope, intercept) and the determination coefficient. This is now explicitly mentioned in section 2.3 (validation framework).
- Figures 6, 7 and 8 and Tables 3, 4, 5 and Tables S.2 to S.8 changed in the current version because we realized that statistics were computed after the removal of the outliers without any mention in the manuscript. This had a minor impact on the statistics which were however corrected.
- MERIS time series has been added to Figure 7 along with the basin coverage increase that is gained with Multi product with respect to the best coverage obtained with the single sensors.
- Figure 5 was corrected to change the name of the Kd algorithm for the Mediterranean from MedOC4 to Medkd.2018. While editing we also recomputed that the Medkd.2018 coefficients (not the functional form).
- A new Table (S.10) has been added in Supplementary Material for the comparison with Chl matchup results from the Climate Assessment Report of the OC-CCI project.

Below is the point-by-point response to the reviews which include a list of all relevant changes made in the newer version of the manuscript. At the end of this file a marked-up manuscript version has also been appended.

Reply to Anonymous Referee #1

We wish to thank Referee #1 for the very detailed and pertinent comments that helped to greatly improve the manuscript. We addressed all the general and specific comments as detailed below with a line-by-line response provided in italic.

In the revised version of the manuscript we will clearly identifying its objectives in line with the CMEMS special issue and the operational oceanography requirements. We will provide more details on the processing chain implementation to clarify several issues pointed out in this review. We will restructure section 2 on data and methods. We will evaluate the effects of the time window on the match-up analyses. We will improve the quality of Figure 1. We will add the validation of Kd using BGCArgo float data with a new figure in the body of the manuscript. We will add new figures in the supplementary materials.

This is the review of the manuscript “The Mediterranean Ocean Colour Level-3 operational multi-sensor processing” by Volpe et al. The paper is mostly a description of the near-real-time/delayed-time processing of ocean color data in the framework of CMEMS. Results are mostly based on a validation analysis. Overall, the text reads more like a project report than a scientific paper, even if intended for a special issue on the European Copernicus Marine Service. It is actually incomplete or confusing in its description of various aspects of the processing (as shown by the list of secondary comments). So the text should be thoroughly reorganized to aim at clear descriptions (starting with the actual objectives of the paper) and the ‘scientific’ part should be reinforced before being considered for publication. These points are further developed below.

As demonstrated by the list of secondary comments, the description of the processing is often unclear and the pertinence of some processing steps is insufficiently supported. I understand that the authors ran into objective difficulties in documenting the processing chain with some elements that are fairly technical and apparently not fully described in literature (bow-tie effect, removing outliers, bias correction, smoothing. . .). I am wondering if some elements are described in more details in CMEMS (or other) reports / ATBDs that could be cited while simplifying the description of technical elements. An alternative is to use this paper as an opportunity to justify the choices made in the various processing steps and focus the work essentially on these. After the ‘technical’ part, the ‘scientific’ part is restricted to 2 pages (out of 13 pages of text) and could easily be reinforced with more discussion (currently there is very little description and discussion of the results, no comparison with published validation results, . . .). Based on the objectives of the paper, the authors should choose which part (‘technical’ or ‘validation) to strengthen.

In the new version of the paper we will highlight the nature of the work by clearly identifying its objectives in line with the CMEMS special issue and the operational oceanography requirements. We will provide more details on the processing chain implementation to clarify several issues pointed out in this review. We will evaluate the effects of the time window on the match-up analyses. We will add the validation of Kd using BGCArgo float data. We will add new figures in the supplementary materials.

Besides the various points listed below, a more general lack of information can be noted when it comes to the comparison of processing chains in the validation analysis, CMEMS processing versus OC-CCI. The paper says that the CMEMS product used for validation is the near-real time (NRT) output. For me, this would mean that the data used in the validation analysis are those obtained in NRT mode, preserved as the processing went (i.e., computed with preliminary ancillary data, calibration at the date of acquisition, with climatology computed with very little data, etc. . .). In

that case validation results reflect the quality of the data as downloaded NRT by users. Otherwise they are DT data, or even fully reprocessed data if they result from a consistent processing all the way through the time period (in terms of calibration, climatology computed with multiple years...). This (and implications) must be made clear in the manuscript (actually, how the validation results evolve as data are brought from NRT to DT and to reprocessed data is an interesting point).

The Reviewer is right. In the revised manuscript we will make clear that the matchup analysis refers to DT data. It would be very interesting to investigate on the quality drift that data may have between NRT and DT. However, since the CMEMS processing chain downloads the Level-2 from space agencies and this work involves the Level-1 to Level-2 processing step, this would require a reprocessing from Level-1 (using the NRT configuration) of all the days involved in the matchup analysis. The current chain is not meant for that.

Besides the mode (NRT, DT) actually associated with the CMEMS data used in the analysis, more discussion should be given comparing those with the CCI data. The manuscript forgets to mention other large differences between the CMEMS and CCI processing, including the atmospheric correction for certain sensors. In the extraction step, the grids of the products are also different (1-km versus 4-km if I am not mistaken). The study should clearly identify all possible sources of differences between the CMEMS and the CCI stream.

We will briefly describe the OC-CCI method with respect to the inter-sensor bias correction and mention the different atmospheric correction for certain sensors. The different spatial resolution was already mentioned in the original submission (page 5, line 7). However, we will rephrase the paragraph to make it more clear.

I have an issue with the field data. They are introduced in the study to explain the MedOC4 algorithm and the validation analysis. In such a context, a word on the uncertainties associated with the data would be necessary. Not clear to me is the distinction between the data serving for the development of MedOC4 and the data used for validation with match-ups (points of the former going into the latter are not fully independent validation points). As they are used for validation, BOUSSOLE and AERONET-OC data should be described a bit better. While I'm not familiar with the BOUSSOLE data distribution, there is a clear data policy for use of the AERONET-OC data (offer of authorship if I'm not mistaken) and I'm wondering if this has been respected (there is not even an acknowledgment in the manuscript).

Figure 1 showing the Cal/Val dataset will be redrawn to better show their distribution, and from which it will appear clear that the calibration data are not being used for validation. The reviewer is right; the section acknowledgement was missing. We will fill it acknowledging AERONET-OC, BOUSSOLE, BGC-Argo and NASA OBPG as those providing high quality data and which we are grateful to. The AERONET-OC PI declined our offer of co-authorship .

Below are detailed comments, with requests for clarification/corrections and suggestions for improving the text. I'd recommend numbering the sections and sub-sections.

We will number all sections and sub-sections.

Page 1

1.10: I'd suggest: "multi-sensor processing applied to the Mediterranean Sea by the Ocean Colour Thematic Assembly Centre of the Copernicus...": The abstract should be readable by readers who don't know about CMEMS, TAC, ...

OK

1.11: “A basin-scale. . .”

OK

1.12: “to fine-tune”

OK

1.14: “than those”

OK

1.15: “The Mediteranean. . .”: information associated with this sentence should be relocated in the beginning of the abstract.

OK

1.21: “CMEMS delivers. . .” rather than ‘includes’

OK

1.27: “users who”

OK

1.28: please define all acronyms at first use.

OK

Page 2

1.2: “near-real time (NRT) and delayed time (DT) modes.”

OK

1.3: in OC jargon, monthly data computed from daily data are still termed L3.

We will add the terms “Within CMEMS” at the beginning of the sentence to stress that this is the current terminology adopted by the Copernicus service.

1.15: is there a reference for this approach?

We will remove the statement from the introduction and add sentence framing this approach in the conclusions.

1.17-18: heavy sentence about 2 important benefits; should be reworded.

We will rephrase and split the sentence.

1.20: “are derived”

OK

1.23: “is foreseen”: so it is still not the case, which is at variance with the abstract.

This sentence refers to OLCI, which is still not included in the multi-sensor product. It will probably be so by 2019. We do not see any discrepancy with what is stated into the Abstract, where OLCI is not mentioned.

1.26: “DT data”

OK

1.26: “precise”: what does this indicate exactly? 1.27: “both to be accurate”: does it mean DT and REP? then the sentence should be restructured. What does ‘consistent’ mean here?

The sentence will be rephrased into “As such, DT data are expected to be as accurate as timeliness allows. The accuracy of REP data need to be stable in time as these data are consistently processed with a single software version.”

1.27: “For the sake of timeliness. . .”

OK

Page 3

1.4: “This work. . .”: this paragraph describes the structure of the work, but the primary objective of the whole study is not clear. Page 2, line 28, “one of the aims” is mentioned, but how does it fit here, and what are the other aims?

We will add a sentence explicitly stating that the overall objective of the work is to provide Copernicus users with a comprehensive description of the method currently applied in the OCTAC context of CMEMS to produce the multi-sensor ocean colour product over the Mediterranean Sea. Propagating the REP configuration to the DT processing mode is part of the method.

1.14: “relies on an in situ. . .”

OK

1.18: odd sentence; it means “absorption due to CDOM, absorption due to algal and non-algal particles, absorption due to TSM, and both AOPs and IOPs.” absorption is part of the IOPs, so which are the others measured? 1.20: are the in-situ IOPs used in this study?

We will rephrase the sentence to avoid confusion and to more clearly specify what are the in situ data that were actually used in this study.

1.30: are the authors sure about the choice of acronym . . . a large part of the scientific community is sufficiently well-versed in latin languages to understand the meaning of the word.

We will change to “Multi-level data processing is achieved using the Software for the Elaboration of Radiometer Data Acquisitions (SERDA)”.

Page 4

1.2: “normalised by”

OK

1.3: Kl and Ku should be defined.

OK

1.9: “using the primary sub-surface quantities, it is then”

OK

1.10: “such as the Q-factor”

OK

1.18: “Chl”: are Chl data from BOUSSOLE used in this work?

Actually they are not. We will remove Chl from the sentence.

Page 5

1.6: “using the OC-CCI. . .”

OK

1.7: this sentence reads: “OC-CCI... at 1-km ... rather than at 4-km for OC-CCI”: unclear.

We will rephrase the entire paragraph.

1.14: “Single-sensor pre-processing for NRT/DT modes” I presume.

It will be changed to ‘NRT/DT single-sensor pre-processing’

1.15: “quality-checked”: what does it entail?

We will add a sentence to briefly explain the kind of data quality checks that are operationally performed.

1.15: I assume that the atmospheric correction applied in these cases is l2gen. This should be mentioned together with an appropriate reference.

We will add a sentence in the previous paragraph to mention that the NRT/DT data are downloaded from the OBPG at NASA that uses the l2gen in its default parameterisation for the L1 to L2 processing. Later in the paragraph we will add similar details for the REP processing.

1.22: “that reflects” . . . “stripes originate”

OK

1.32: “the dimension . . .”: it happens also for the other sensors, doesn’t it?

Yes. We will rephrase the paragraph to make it clear.

Page 6

1.2: “these missing values”: what is the benefit of this step?

We will specify that the benefit is particularly evident in view of the sensor merging.

1.6: and what about SeaWiFS and MERIS?

To generalize we removed the reference to MODIS-AQUA and VIIRS. Please see also response to comment P7.L7

1.6: “space agencies”: in that case it is only NASA.

OK

1.7: “atmospheric correction failure”: this is a strong step; I would assume that Rrs associated with that flag is just not usable as the AC failed according to the software. What is the criterion used by the software to consider the AC a ‘failure’? what is then the status of Rrs? The authors should also support this decision with robust evidence that the resulting Rrs is actually valid.

We will add details on the processing of pixels identified through the bowtie removal flag. We will clarify that the atmospheric correction failure flag is not applied to VIIRS because it overlaps with the bowtie removal flag for almost all water pixels. We tested the 645 granules (each of 3200x3232 pixels) acquired over the Mediterranean Sea in 100 days (10 April 2018 to 18 July 2018) and found that only in 31 pixels the atmospheric correction failure flag was raised for pixels not affected by bow tie deletion or any of the other OBPG standard flags.

1.8: “to avoid”

OK

1.8: “salt and pepper”: please define what this refers to.

OK

1.9: “removing all isolated pixels...”: in general, this part needs clearer explanation. How is an “isolated pixel” defined?

We will add a sentence to specify the meaning of the isolated pixel.

1.13: please provide characteristics of the map (extent, resolution).

OK

1.17: “spectra” from different missions?

Yes. We actually wrote “to merge single-sensor Rrs spectra into a single spectrum”. Adding from “different missions” would be redundant.

1.21: “differ by”

OK

1.25: “In general”: may be removed.

OK

1.30: “in theory”: and in practice? Might be removed.

OK

1.31: “apply algorithms to derive geophysical products”

OK

Page 7

1.3-5: not clear what the idea is here.

We will remove this sentence.

1.7: “Differences between MODIS and VIIRS”; and what about SeaWiFS and MERIS? In general some aspects of the manuscript associated with NRT/DT seem focused exclusively on MODIS/VIIRS (that has some logic since they are still active) but how SeaWiFS and MERIS are handled should also be described as the related products are used in the validation analysis.

We will add a sentence in section 2.2 (satellite data processing chain) to clarify that the current NRT/DT processing only involves MODIS-AQUA and VIIRS platforms, and that for the sole scope of the product validation we used the Multi-sensor production chain described in that section (2.2) to process the entire satellite data archive from 1997, thus including SeaWiFS and MERIS data.

1.11: “normalized”: does the BRDF correction make use of the OCI Chla value? In that, it is not consistent with the MedOC4 values. This should be acknowledged.

We will add a sentence acknowledging the issue in the result section when commenting the Rrs matchup analysis, focusing on the trade-offs between accuracy and timeliness in the operational oceanography framework. Furthermore, this issue will be also the topic of a new paragraph discussing the the accuracy of Rrs in section 4.

1.17: “we tested”: by doing what? 1.19: “inter-calibration”: it is certainly a factor but it is not the only one that could apply. I would still argue that geometry can play a significant role in the differences. Operating the atmospheric correction with different bands might also have an impact through the AC code (eliciting different responses by the AC code and its assumptions/simplifications).

At pixel scale, the cosine of the scattering angle was compared with the ratio between MODIS-AQUA and VIIRS Rrs for each band. As it will be shown by the new figure in Supplementary Material, no specific pattern was evident through this analysis. We will acknowledge that there might be some other factors linked to the AC influencing the difference between sensors.

1.22: it does not seem that the bias correction operated by CCI is described in that reference.

OK, reference will be corrected. This paragraph will be partially rewritten to address the series of comments below about the implemented bias-correction method.

1.25: “climatological”: what are the periods used for each sensor? is it the same?

1.28: “two steps”: but then 3 are listed. 1.29: “temporary”? Page 8: 1.1: aren’t the same equations used by CCI? 1.5: “weight w” 1.8: “and time”: not necessary. 1.8: “as for OC-CCI”: this should be written before. I think CCI also operates some type of spatial averaging.

1.12: “deemed insufficient”: on the basis of what?

One of the output of Figure 6 is that the performances of SeaWiFS at 670 nm were the worst as compared with the other bands and sensors. This justifies the choice of not using this sensor band as reference for bias adjusting the other sensors. This sentence will be rephrased.

1.13: “40%”: what is the reason for so many missing values at 670 nm? Negative values? But earlier in the text, it is written that the quality check removes all incomplete spectra (if Rrs is <0 at any one band). So at that point, working with incomplete spectra for match-ups is inconsistent with the processing chain.

In the “Flagging & Mosaicking” paragraph, we will correct “one negative value within the spectrum (excluding the NIR bands) is enough for the entire spectrum to be rejected” replacing NIR with 670nm.

1.22: which “method”?

We will replace “method” with “merging”.

1.24: “are only the result of the merging procedure”

OK

1.26-29: I have to say that I don’t understand how the approach works. Volpe et al. (2018) not being published, the explanation should be clearer. For instance, is the climatology field computed as in the previous section? And then it is not clear how the smoothing operates.

We will rephrase the sentence into “To prevent the occurrence of such horizontal discontinuities, here we apply the smoothing procedure described in Volpe et al. (2018) and based on the use of the climatology field, described below”. Volpe et al. (2018) is now published. We will also add a few sentences to better explain how the smoothing operates.

Page 9

1.2-8: The examples are not so obvious to me. I don’t even see the Rhone plume on any map (should be a pattern leaving the coast. . .).

We will add labels on Figure 3e to ease the reading.

1.12: “In both cases”: this is true for the cases shown but is it a general result? In any case, there is no reason to expect that the bias-corrected merged data would be closer to the field data than a simple average.

The validation results of Figure 6 show that this is a general result.

1.15: “The climatology field is obtained. . .”: climatology is also mentioned in the 2 previous sections (bias correction, merging), so it is not clear what this SeaWiFS Chla climatology is for, nor why it is computed in a different way.

We will make a clear difference between the daily climatology bias map used in the context of the bias correction and the field climatology used for the sensor merging. We will also remove the incorrect bit “using the MedOC4 regional algorithm for CHL (Volpe et al., 2007)”. We will add a sentence to mention that the next version of the processing chain will include a climatology field

computed following the method adopted in the bias correction section.

1.20: “this has been estimated”: how? (or where?)

We will add the appropriate reference.

1.22: “To overcome . . .”: but this type of filtering was already introduced for the Level-2 data. Do outliers appear again later in the processing ? Speaking of ‘biases’ here is not appropriate.

Since it is mentioned earlier in the manuscript, we will remove this part from this context.

1.32: “Even though the latter now show performance comparable to that of empirical algorithms. . .”

OK

Page 10

1.1: “in discussing the characteristics that data must have to be used. . .”

OK

1.2: “pointed out that . . .”: the sentence should be re-written.

We will rephrase the sentence

1.2: “theoretical”: to be replaced by ‘semi-analytical’ (what is a theoretical algorithm?)

OK

1.10: “weather conditions”

OK

1.15: “To identify. . . the identification. . .”: sentence to be re-written.

We will rephrase the sentence.

1.17: “average spectra”: the covariance matrix is also needed for such an approach.

We will add the necessary details to the sentence.

1.21: “user survey”: refers to the CCI user consultation?

Yes, we will change it.

1.6-24: in general I think this paragraph may be too long as the approach has already been well described in literature. Regardless of length I don’t find it clear for a reader without a prior knowledge of the method.

We hope that after the suggested changes the paragraph will read better.

Page 11

1.12: “unable to perform”

We will add the results of validation analysis performed using the BGC-Argo float L3 data (Organelli et al., 2017, Earth Syst. Sci. Data).

1.15: “Inherent Optical Properties”: I was therefore expecting validation results for the IOPs while there are none.

We will remove the IOPs from this sentence. A reference to the Pitarch et 2016 al for the assessment of QAA based bbp in the the Mediterranean Sea will be added in the methods section at 2.2.1 where the use of QAA is first described.

1.18: “in most instances”: some example stats would be appropriate.

We will rephrase this sentence to show that the overall validation results are not significantly affected by the temporal window. We will add a new figure in Supplementary Material to show the statistics behaviour with a variable temporal window.

Page 12:

1.2: “used the NRT”: meaning data processed as they were in NRT conditions (with preliminary ancillary data, calibration known at the time of acquisition, preliminary climatology, etc. . .)?

We will correct NRT into NRT/DT. As mentioned earlier, we will add a couple of sentences in Section 2.2 (Satellite Data Processing Chain) where we better explain the differences between NRT and DT data and that for the sole scope of the product validation we used the NRT/DT production chain described in that section (2.2) to process the entire satellite data archive from 1997, thus including SeaWiFS and MERIS data.

1.12: “common spectral behaviour”: is this a point that could be discussed?

We will add some discussion on this point.

1.18: “significantly”: was any statistical test performed?

No, we did not perform any statistical tests. However, “do not significantly differ” here referred to the fact that the standard deviation bars in Figure 6 do overlap to one another. We will rephrase the statement by replacing “significantly” with “substantially”.

Page 13

1.4: “significant”; what does it mean here?

We will change “significant” to “relevant”.

1.5: “In the NIR”: in the red?

OK

Table 4: why are there less matchups at 670 nm (I understood that only complete spectra were kept)? The fact that the Multi and CCI products have a different number of match-ups should be discussed.

In the revised version of the manuscript we will expand on this.

1.12: “NRT”: or DT?

We will correct to NRT/DT.

Figure 1: not so easy to distinguish validation from development points.

We will make it better

Figure 3: remind that the climatology fields are from a daily climatology.

OK

Figure 5: “Pope and Fry 1972”?

Corrected to Mueller (2000).

Table 5: writes ‘REP’ versus ‘Multi’ while Table writes ‘CCI’ versus ‘Multi’; coherence is needed to avoid confusion. While Table 4 shows different numbers of match-ups for the 2 products, here the numbers are the same. Is there an explanation for this?

A thorough check throughout the manuscript will ensure consistency of the use of REP to identify the dataset and CCIv3 to identify the source processing chain for Rrs.

Reply to Anonymous Referee #1

We wish to thank Referee #1 for the very detailed and pertinent comments that helped to greatly improve the manuscript. We addressed all the general and specific comments as detailed below with a line-by-line response provided in italic.

In the revised version of the manuscript we will clearly identifying its objectives in line with the CMEMS special issue and the operational oceanography requirements. We will provide more details on the processing chain implementation to clarify several issues pointed out in this review. We will restructure section 2 on data and methods. We will evaluate the effects of the time window on the match-up analyses. We will improve the quality of Figure 1. We will add the validation of Kd using BGCArgo float data with a new figure in the body of the manuscript. We will add new figures in the supplementary materials.

This is the review of the manuscript “The Mediterranean Ocean Colour Level-3 operational multi-sensor processing” by Volpe et al. The paper is mostly a description of the near-real-time/delayed-time processing of ocean color data in the framework of CMEMS. Results are mostly based on a validation analysis. Overall, the text reads more like a project report than a scientific paper, even if intended for a special issue on the European Copernicus Marine Service. It is actually incomplete or confusing in its description of various aspects of the processing (as shown by the list of secondary comments). So the text should be thoroughly reorganized to aim at clear descriptions (starting with the actual objectives of the paper) and the ‘scientific’ part should be reinforced before being considered for publication. These points are further developed below.

As demonstrated by the list of secondary comments, the description of the processing is often unclear and the pertinence of some processing steps is insufficiently supported. I understand that the authors ran into objective difficulties in documenting the processing chain with some elements that are fairly technical and apparently not fully described in literature (bow-tie effect, removing outliers, bias correction, smoothing. . .). I am wondering if some elements are described in more details in CMEMS (or other) reports / ATBDs that could be cited while simplifying the description of technical elements. An alternative is to use this paper as an opportunity to justify the choices made in the various processing steps and focus the work essentially on these. After the ‘technical’ part, the ‘scientific’ part is restricted to 2 pages (out of 13 pages of text) and could easily be reinforced with more discussion (currently there is very little description and discussion of the results, no comparison with published validation results, . . .). Based on the objectives of the paper, the authors should choose which part (‘technical’ or ‘validation) to strengthen.

In the new version of the paper we will highlight the nature of the work by clearly identifying its objectives in line with the CMEMS special issue and the operational oceanography requirements. We will provide more details on the processing chain implementation to clarify several issues pointed out in this review. We will evaluate the effects of the time window on the match-up analyses. We will add the validation of Kd using BGCArgo float data. We will add new figures in the supplementary materials.

Besides the various points listed below, a more general lack of information can be noted when it comes to the comparison of processing chains in the validation analysis, CMEMS processing versus OC-CCI. The paper says that the CMEMS product used for validation is the near-real time (NRT) output. For me, this would mean that the data used in the validation analysis are those obtained in NRT mode, preserved as the processing went (i.e., computed with preliminary ancillary data, calibration at the date of acquisition, with climatology computed with very little data, etc. . .). In

that case validation results reflect the quality of the data as downloaded NRT by users. Otherwise they are DT data, or even fully reprocessed data if they result from a consistent processing all the way through the time period (in terms of calibration, climatology computed with multiple years...). This (and implications) must be made clear in the manuscript (actually, how the validation results evolve as data are brought from NRT to DT and to reprocessed data is an interesting point).

The Reviewer is right. In the revised manuscript we will make clear that the matchup analysis refers to DT data. It would be very interesting to investigate on the quality drift that data may have between NRT and DT. However, since the CMEMS processing chain downloads the Level-2 from space agencies and this work involves the Level-1 to Level-2 processing step, this would require a reprocessing from Level-1 (using the NRT configuration) of all the days involved in the matchup analysis. The current chain is not meant for that.

Besides the mode (NRT, DT) actually associated with the CMEMS data used in the analysis, more discussion should be given comparing those with the CCI data. The manuscript forgets to mention other large differences between the CMEMS and CCI processing, including the atmospheric correction for certain sensors. In the extraction step, the grids of the products are also different (1-km versus 4-km if I am not mistaken). The study should clearly identify all possible sources of differences between the CMEMS and the CCI stream.

We will briefly describe the OC-CCI method with respect to the inter-sensor bias correction and mention the different atmospheric correction for certain sensors. The different spatial resolution was already mentioned in the original submission (page 5, line 7). However, we will rephrase the paragraph to make it more clear.

I have an issue with the field data. They are introduced in the study to explain the MedOC4 algorithm and the validation analysis. In such a context, a word on the uncertainties associated with the data would be necessary. Not clear to me is the distinction between the data serving for the development of MedOC4 and the data used for validation with match-ups (points of the former going into the latter are not fully independent validation points). As they are used for validation, BOUSSOLE and AERONET-OC data should be described a bit better. While I'm not familiar with the BOUSSOLE data distribution, there is a clear data policy for use of the AERONET-OC data (offer of authorship if I'm not mistaken) and I'm wondering if this has been respected (there is not even an acknowledgment in the manuscript).

Figure 1 showing the Cal/Val dataset will be redrawn to better show their distribution, and from which it will appear clear that the calibration data are not being used for validation. The reviewer is right; the section acknowledgement was missing. We will fill it acknowledging AERONET-OC, BOUSSOLE, BGC-Argo and NASA OBPG as those providing high quality data and which we are grateful to. The AERONET-OC PI declined our offer of co-authorship .

Below are detailed comments, with requests for clarification/corrections and suggestions for improving the text. I'd recommend numbering the sections and sub-sections.

We will number all sections and sub-sections.

Page 1

1.10: I'd suggest: "multi-sensor processing applied to the Mediterranean Sea by the Ocean Colour Thematic Assembly Centre of the Copernicus...": The abstract should be readable by readers who don't know about CMEMS, TAC, ...

OK

1.11: “A basin-scale. . .”

OK

1.12: “to fine-tune”

OK

1.14: “than those”

OK

1.15: “The Mediteranean. . .”: information associated with this sentence should be relocated in the beginning of the abstract.

OK

1.21: “CMEMS delivers. . .” rather than ‘includes’

OK

1.27: “users who”

OK

1.28: please define all acronyms at first use.

OK

Page 2

1.2: “near-real time (NRT) and delayed time (DT) modes.”

OK

1.3: in OC jargon, monthly data computed from daily data are still termed L3.

We will add the terms “Within CMEMS” at the beginning of the sentence to stress that this is the current terminology adopted by the Copernicus service.

1.15: is there a reference for this approach?

We will remove the statement from the introduction and add sentence framing this approach in the conclusions.

1.17-18: heavy sentence about 2 important benefits; should be reworded.

We will rephrase and split the sentence.

1.20: “are derived”

OK

1.23: “is foreseen”: so it is still not the case, which is at variance with the abstract.

This sentence refers to OLCI, which is still not included in the multi-sensor product. It will probably be so by 2019. We do not see any discrepancy with what is stated into the Abstract, where OLCI is not mentioned.

1.26: “DT data”

OK

1.26: “precise”: what does this indicate exactly? 1.27: “both to be accurate”: does it mean DT and REP? then the sentence should be restructured. What does ‘consistent’ mean here?

The sentence will be rephrased into “As such, DT data are expected to be as accurate as timeliness allows. The accuracy of REP data need to be stable in time as these data are consistently processed with a single software version.”

1.27: “For the sake of timeliness. . .”

OK

Page 3

1.4: “This work. . .”: this paragraph describes the structure of the work, but the primary objective of the whole study is not clear. Page 2, line 28, “one of the aims” is mentioned, but how does it fit here, and what are the other aims?

We will add a sentence explicitly stating that the overall objective of the work is to provide Copernicus users with a comprehensive description of the method currently applied in the OCTAC context of CMEMS to produce the multi-sensor ocean colour product over the Mediterranean Sea. Propagating the REP configuration to the DT processing mode is part of the method.

1.14: “relies on an in situ. . .”

OK

1.18: odd sentence; it means “absorption due to CDOM, absorption due to algal and non-algal particles, absorption due to TSM, and both AOPs and IOPs.” absorption is part of the IOPs, so which are the others measured? 1.20: are the in-situ IOPs used in this study?

We will rephrase the sentence to avoid confusion and to more clearly specify what are the in situ data that were actually used in this study.

1.30: are the authors sure about the choice of acronym . . . a large part of the scientific community is sufficiently well-versed in latin languages to understand the meaning of the word.

We will change to “Multi-level data processing is achieved using the Software for the Elaboration of Radiometer Data Acquisitions (SERDA)”.

Page 4

1.2: “normalised by”

OK

1.3: Kl and Ku should be defined.

OK

1.9: “using the primary sub-surface quantities, it is then”

OK

1.10: “such as the Q-factor”

OK

1.18: “Chl”: are Chl data from BOUSSOLE used in this work?

Actually they are not. We will remove Chl from the sentence.

Page 5

1.6: “using the OC-CCI. . .”

OK

1.7: this sentence reads: “OC-CCI... at 1-km ... rather than at 4-km for OC-CCI”: unclear.

We will rephrase the entire paragraph.

1.14: “Single-sensor pre-processing for NRT/DT modes” I presume.

It will be changed to ‘NRT/DT single-sensor pre-processing’

1.15: “quality-checked”: what does it entail?

We will add a sentence to briefly explain the kind of data quality checks that are operationally performed.

1.15: I assume that the atmospheric correction applied in these cases is l2gen. This should be mentioned together with an appropriate reference.

We will add a sentence in the previous paragraph to mention that the NRT/DT data are downloaded from the OBPG at NASA that uses the l2gen in its default parameterisation for the L1 to L2 processing. Later in the paragraph we will add similar details for the REP processing.

1.22: “that reflects” . . . “stripes originate”

OK

1.32: “the dimension . . .”: it happens also for the other sensors, doesn’t it?

Yes. We will rephrase the paragraph to make it clear.

Page 6

1.2: “these missing values”: what is the benefit of this step?

We will specify that the benefit is particularly evident in view of the sensor merging.

1.6: and what about SeaWiFS and MERIS?

To generalize we removed the reference to MODIS-AQUA and VIIRS. Please see also response to comment P7.L7

1.6: “space agencies”: in that case it is only NASA.

OK

1.7: “atmospheric correction failure”: this is a strong step; I would assume that Rrs associated with that flag is just not usable as the AC failed according to the software. What is the criterion used by the software to consider the AC a ‘failure’? what is then the status of Rrs? The authors should also support this decision with robust evidence that the resulting Rrs is actually valid.

We will add details on the processing of pixels identified through the bowtie removal flag. We will clarify that the atmospheric correction failure flag is not applied to VIIRS because it overlaps with the bowtie removal flag for almost all water pixels. We tested the 645 granules (each of 3200x3232 pixels) acquired over the Mediterranean Sea in 100 days (10 April 2018 to 18 July 2018) and found that only in 31 pixels the atmospheric correction failure flag was raised for pixels not affected by bow tie deletion or any of the other OBPG standard flags.

1.8: “to avoid”

OK

1.8: “salt and pepper”: please define what this refers to.

OK

1.9: “removing all isolated pixels...”: in general, this part needs clearer explanation. How is an “isolated pixel” defined?

We will add a sentence to specify the meaning of the isolated pixel.

1.13: please provide characteristics of the map (extent, resolution).

OK

1.17: “spectra” from different missions?

Yes. We actually wrote “to merge single-sensor Rrs spectra into a single spectrum”. Adding from “different missions” would be redundant.

1.21: “differ by”

OK

1.25: “In general”: may be removed.

OK

1.30: “in theory”: and in practice? Might be removed.

OK

1.31: “apply algorithms to derive geophysical products”

OK

Page 7

1.3-5: not clear what the idea is here.

We will remove this sentence.

1.7: “Differences between MODIS and VIIRS”; and what about SeaWiFS and MERIS? In general some aspects of the manuscript associated with NRT/DT seem focused exclusively on MODIS/VIIRS (that has some logic since they are still active) but how SeaWiFS and MERIS are handled should also be described as the related products are used in the validation analysis.

We will add a sentence in section 2.2 (satellite data processing chain) to clarify that the current NRT/DT processing only involves MODIS-AQUA and VIIRS platforms, and that for the sole scope of the product validation we used the Multi-sensor production chain described in that section (2.2) to process the entire satellite data archive from 1997, thus including SeaWiFS and MERIS data.

1.11: “normalized”: does the BRDF correction make use of the OCI Chla value? In that, it is not consistent with the MedOC4 values. This should be acknowledged.

We will add a sentence acknowledging the issue in the result section when commenting the Rrs matchup analysis, focusing on the trade-offs between accuracy and timeliness in the operational oceanography framework. Furthermore, this issue will be also the topic of a new paragraph discussing the the accuracy of Rrs in section 4.

1.17: “we tested”: by doing what? 1.19: “inter-calibration”: it is certainly a factor but it is not the only one that could apply. I would still argue that geometry can play a significant role in the differences. Operating the atmospheric correction with different bands might also have an impact through the AC code (eliciting different responses by the AC code and its assumptions/simplifications).

At pixel scale, the cosine of the scattering angle was compared with the ratio between MODIS-AQUA and VIIRS Rrs for each band. As it will be shown by the new figure in Supplementary Material, no specific pattern was evident through this analysis. We will acknowledge that there might be some other factors linked to the AC influencing the difference between sensors.

1.22: it does not seem that the bias correction operated by CCI is described in that reference.

OK, reference will be corrected. This paragraph will be partially rewritten to address the series of comments below about the implemented bias-correction method.

1.25: “climatological”: what are the periods used for each sensor? is it the same?

1.28: “two steps”: but then 3 are listed. 1.29: “temporary”? Page 8: 1.1: aren’t the same equations used by CCI? 1.5: “weight w” 1.8: “and time”: not necessary. 1.8: “as for OC-CCI”: this should be written before. I think CCI also operates some type of spatial averaging.

1.12: “deemed insufficient”: on the basis of what?

One of the output of Figure 6 is that the performances of SeaWiFS at 670 nm were the worst as compared with the other bands and sensors. This justifies the choice of not using this sensor band as reference for bias adjusting the other sensors. This sentence will be rephrased.

1.13: “40%”: what is the reason for so many missing values at 670 nm? Negative values? But earlier in the text, it is written that the quality check removes all incomplete spectra (if Rrs is <0 at any one band). So at that point, working with incomplete spectra for match-ups is inconsistent with the processing chain.

In the “Flagging & Mosaicking” paragraph, we will correct “one negative value within the spectrum (excluding the NIR bands) is enough for the entire spectrum to be rejected” replacing NIR with 670nm.

1.22: which “method”?

We will replace “method” with “merging”.

1.24: “are only the result of the merging procedure”

OK

1.26-29: I have to say that I don’t understand how the approach works. Volpe et al. (2018) not being published, the explanation should be clearer. For instance, is the climatology field computed as in the previous section? And then it is not clear how the smoothing operates.

We will rephrase the sentence into “To prevent the occurrence of such horizontal discontinuities, here we apply the smoothing procedure described in Volpe et al. (2018) and based on the use of the climatology field, described below”. Volpe et al. (2018) is now published. We will also add a few sentences to better explain how the smoothing operates.

Page 9

1.2-8: The examples are not so obvious to me. I don’t even see the Rhone plume on any map (should be a pattern leaving the coast. . .).

We will add labels on Figure 3e to ease the reading.

1.12: “In both cases”: this is true for the cases shown but is it a general result? In any case, there is no reason to expect that the bias-corrected merged data would be closer to the field data than a simple average.

The validation results of Figure 6 show that this is a general result.

1.15: “The climatology field is obtained. . .”: climatology is also mentioned in the 2 previous sections (bias correction, merging), so it is not clear what this SeaWiFS Chla climatology is for, nor why it is computed in a different way.

We will make a clear difference between the daily climatology bias map used in the context of the bias correction and the field climatology used for the sensor merging. We will also remove the incorrect bit “using the MedOC4 regional algorithm for CHL (Volpe et al., 2007)”. We will add a sentence to mention that the next version of the processing chain will include a climatology field

computed following the method adopted in the bias correction section.

1.20: “this has been estimated”: how? (or where?)

We will add the appropriate reference.

1.22: “To overcome . . .”: but this type of filtering was already introduced for the Level-2 data. Do outliers appear again later in the processing ? Speaking of ‘biases’ here is not appropriate.

Since it is mentioned earlier in the manuscript, we will remove this part from this context.

1.32: “Even though the latter now show performance comparable to that of empirical algorithms. . .”

OK

Page 10

1.1: “in discussing the characteristics that data must have to be used. . .”

OK

1.2: “pointed out that . . .”: the sentence should be re-written.

We will rephrase the sentence

1.2: “theoretical”: to be replaced by ‘semi-analytical’ (what is a theoretical algorithm?)

OK

1.10: “weather conditions”

OK

1.15: “To identify. . . the identification. . .”: sentence to be re-written.

We will rephrase the sentence.

1.17: “average spectra”: the covariance matrix is also needed for such an approach.

We will add the necessary details to the sentence.

1.21: “user survey”: refers to the CCI user consultation?

Yes, we will change it.

1.6-24: in general I think this paragraph may be too long as the approach has already been well described in literature. Regardless of length I don’t find it clear for a reader without a prior knowledge of the method.

We hope that after the suggested changes the paragraph will read better.

Page 11

1.12: “unable to perform”

We will add the results of validation analysis performed using the BGC-Argo float L3 data (Organelli et al., 2017, Earth Syst. Sci. Data).

1.15: “Inherent Optical Properties”: I was therefore expecting validation results for the IOPs while there are none.

We will remove the IOPs from this sentence. A reference to the Pitarch et 2016 al for the assessment of QAA based bbp in the the Mediterranean Sea will be added in the methods section at 2.2.1 where the use of QAA is first described.

1.18: “in most instances”: some example stats would be appropriate.

We will rephrase this sentence to show that the overall validation results are not significantly affected by the temporal window. We will add a new figure in Supplementary Material to show the statistics behaviour with a variable temporal window.

Page 12:

1.2: “used the NRT”: meaning data processed as they were in NRT conditions (with preliminary ancillary data, calibration known at the time of acquisition, preliminary climatology, etc. . .)?

We will correct NRT into NRT/DT. As mentioned earlier, we will add a couple of sentences in Section 2.2 (Satellite Data Processing Chain) where we better explain the differences between NRT and DT data and that for the sole scope of the product validation we used the NRT/DT production chain described in that section (2.2) to process the entire satellite data archive from 1997, thus including SeaWiFS and MERIS data.

1.12: “common spectral behaviour”: is this a point that could be discussed?

We will add some discussion on this point.

1.18: “significantly”: was any statistical test performed?

No, we did not perform any statistical tests. However, “do not significantly differ” here referred to the fact that the standard deviation bars in Figure 6 do overlap to one another. We will rephrase the statement by replacing “significantly” with “substantially”.

Page 13

1.4: “significant”; what does it mean here?

We will change “significant” to “relevant”.

1.5: “In the NIR”: in the red?

OK

Table 4: why are there less matchups at 670 nm (I understood that only complete spectra were kept)? The fact that the Multi and CCI products have a different number of match-ups should be discussed.

In the revised version of the manuscript we will expand on this.

1.12: “NRT”: or DT?

We will correct to NRT/DT.

Figure 1: not so easy to distinguish validation from development points.

We will make it better

Figure 3: remind that the climatology fields are from a daily climatology.

OK

Figure 5: “Pope and Fry 1972”?

Corrected to Mueller (2000).

Table 5: writes ‘REP’ versus ‘Multi’ while Table writes ‘CCI’ versus ‘Multi’; coherence is needed to avoid confusion. While Table 4 shows different numbers of match-ups for the 2 products, here the numbers are the same. Is there an explanation for this?

A thorough check throughout the manuscript will ensure consistency of the use of REP to identify the dataset and CCIv3 to identify the source processing chain for Rrs.

Reply to Anonymous Referee #2

We wish to thank Referee #2 for the positive feedback. We addressed the comments as detailed below with a line-by-line response provided in italic.

1. It is understood that the current product merging strategy follows the OC-CCI approach. Please explain whether moving to the Copernicus baseline of spectral band selection for the radiometry is planned in the future.

We will surely comment on this and say that we periodically check upstream data quality by comparison with in situ observations. The outcome of the comparison constitutes the basis for taking any sort of such kinds of decisions. We currently use SeaWiFS as it revealed to be the best sensor in the satellite-in situ data comparison. We will comment on the fact that using a sensor reference means to choose between the need of having the best available quality (e.g., SeaWiFS, in our current case) and to account for the climate-change issue referring to more recent observations (e.g., Copernicus missions).

2. Future evolution to incorporate Copernicus missions, i.e. S3 OLCI (when ready), should also be brought up and discussed.

We will comment on this in the next version of the paper. We will mention that, as stated above, we periodically check the impact of ingesting new data sources into the processing chain when they become available. Moreover, it is important to mention that the evolution quality of new sensors to be ingested into the multi-sensor processing chain is also checked in terms of output data quality and in terms of number of observations available to users.

The Mediterranean Ocean Colour Level 3 Operational Multi-Sensor Processing

Gianluca Volpe¹, Simone Colella¹, Vittorio E. Brando¹, Vega Forneris¹, Flavio La Padula¹, Annalisa Di Cicco¹, Michela Sammartino¹, Marco Bracaglia^{1,2}, Florinda Artuso³, Rosalia Santoleri¹

¹ Istituto di Scienze Marine, Via Fosso del Cavaliere 100, 00133, Roma, Italy

² Università degli Studi di Napoli Parthenope, Via Amm. F. Acton 38, 80133, Naples, Italy

³ Agenzia nazionale per le nuove tecnologie, l'energia e lo sviluppo economico sostenibile, Dipartimento Ambiente, Centro Ricerche Frascati, Frascati, Italy

Correspondence to: Gianluca Volpe (gianluca.volpe@cnr.it)

10 Abstract. The Mediterranean near-real-time multi-sensor processing chain has been set up and is operational in the framework of the Copernicus Marine Environment Monitoring Service (CMEMS). This work describes the main steps operatively performed to enable single ocean colour sensors to enter the multi-sensor processing applied to the Mediterranean Sea by the Ocean Colour Thematic Assembly within CMEMS. Here, the multi-sensor chain takes care of reducing the inter-sensor bias before data from different sensors are merged together. A basin-scale in situ bio-optical 15 dataset is used both to fine-tune the algorithms for the retrieval of phytoplankton chlorophyll and attenuation coefficient of light, k_d , and to assess the uncertainty associated with them. The satellite multi-sensor remote sensing Reflectance spectra better agree with the in situ observations than those of the single sensors. Here we demonstrate that the near-real time processing chain compares sufficiently well with the historical in situ datasets to be confidently used also for reprocessing the full data time series.

20 1 Introduction

The Copernicus Marine Environment Monitoring Service (CMEMS) is one of the six services of the Copernicus program. It provides regular and systematic reference information on the physical state, variability and dynamics of the ocean, ice and marine ecosystems for the global ocean and the European seas. CMEMS delivers both satellite and in-situ high-level products prepared by Thematic Assembly Centres (TACs) and modelling and data assimilation products prepared by

25 Monitoring and Forecasting Centres (MFCs). The Ocean Colour Thematic Assembly Centre (OCTAC) builds and operates the European ocean colour operational service within CMEMS providing global, Pan-European and regional (Arctic Ocean, Atlantic Ocean, Baltic Sea, Black Sea, and Mediterranean Sea) ocean colour (OC) products based on earth observation from OC missions (Le Traou 2015, Von Schuckman 2017). The OCTAC bridges the gap between space agencies, providing ocean colour data, and all users who need the added-value information not available from space agencies. Presently, the OCTAC 30 relies on current and legacy OC sensors: MERIS (MEdium Resolution Imaging Spectrometer) from ESA, SeaWiFS (Sea-

Deleted: dell'Atmosfera e del Clima

Deleted: Ente per le Nuove tecnologie l'Energia e l'Ambiente,

Moved (insertion) [1]

Deleted: processing

Deleted: of the Copernicus Marine Environment Monitoring Service

Deleted: multi-sensor chain for the Mediterranean Sea of Ocean Colour Thematic Assembling Centre

Deleted: The

Deleted: ing

Deleted: Kd

Deleted: that

Deleted: and are comparable with the ESA-OC-CCI multi-sensor product, highlighting the importance of reducing the inter-sensor bias

Deleted:

Moved up [1]: The Mediterranean near-real-time multi-sensor processing chain has been set up and is operational in the framework of the Copernicus Marine Environment Monitoring Service.

Deleted: includes

Deleted: that

Deleted: ,

viewing Wide Field-of-view Sensor) and MODIS (Moderate Resolution Imaging Spectroradiometer) from NASA, VIIRS (Visible Infrared Imager Radiometer Suite) from NOAA, and most recently on the Copernicus Sentinel 3A OLCI (Ocean and Land Colour Instrument) sensor.

Starting from the Level-2 (L2) data downloaded from space agencies, the OCTAC generates Level-3 (L3) and Level-4 (L4)

- 5 products in near-real time (NRT) and delayed time (DT) modes. Within CMEMS, L3 products refer to the single snapshot, or daily combined products, mapped onto a regular grid, while L4 are products for which a temporal averaging method and/or an interpolation procedure is applied to fill in missing data values. The NRT products are operationally produced daily to provide the best estimate of the ocean colour variables at the time of processing. These products are generated soon after the satellite swaths are available together with climatological ancillary data, e.g., meteorological and ozone data for
10 atmospheric correction, and predicted attitude and ephemerides for data geolocation. In the DT processing, the updated ancillary data made available from the space agencies are used to improve the quality of the NRT data. NRT and DT data streams hence are designed to fulfil the operational oceanography specific requirements for near real time availability of high quality satellite data with a sufficiently dense space and time sampling (e.g., Le Traon et al., 2015). Generally, once a year, the full data time series undergoes a reprocessing (REP) to ensure most recent findings to be consistently applied and back
15 propagated to all data. REP products are multi-year time series produced with a consolidated and consistent input dataset and processing software configuration, resulting in a dataset suitable for long-term analyses and climate studies (Von Schuckman et al., 2017, Sathyendranath et al., 2017 and references therein).

Within CMEMS, observations from multiple missions are processed together to ensure homogenized and inter-calibrated datasets for all essential ocean variables. Combining the observations from different platforms results in higher coverage as compared with those of the single sensors. Moreover, the multi-sensor product allows non-expert users to access a robust and less ambiguous source of information. Currently in the OCTAC, the NRT and DT multi-sensor L3 and L4 products are derived from MODIS-AQUA and NPP-VIIRS data, while REP includes observations from SeaWiFS, MODIS-AQUA, MERIS and NPP-VIIRS. Global REP products are derived from two datasets: the OC-CCI (Climate Change Initiative, www.esa-oceancolour-cci.org) funded by the European Space Agency and the Copernicus-GlobColour initially developed
25 by Globcolour Project (www.globcolour.info) and then updated and produced in the framework of CMEMS. OLCI is foreseen to be included into the NRT/DT multi-sensor products in 2019 and in the REP when the quality of the data will be deemed suitable.

In general, DT and REP products are meant to answer different questions and to satisfy different needs such as assimilation into operational models and climate studies, respectively. As such, DT data are expected to be as accurate as timeliness allows. The accuracy of REP data need to be stable in time as these data, which are consistently processed with a single software version, are used for studying long time scale phenomena. For the sake of timeliness, the accuracy of the NRT-DT data is relaxed with respect to the one associated with REP time series. In this respect, one of the aims of this work is to propagate the REP configuration to the DT processing mode, allowing full compatibility between the two datasets and to extend the climate-fit-research to the most recent observations.

Deleted:

Deleted: following the “One Question One Answer” approach of operational satellite oceanography,

Deleted: Moreover, multi-sensor products benefit of a

Deleted: also providing users with

Deleted: as compared with the single-sensor approach

Deleted: 2018

Deleted: As such DT need to be timely and precise while REP data are expected to be stable in time, consistent and both to be accurate.

Deleted: In name

Deleted: the

Regional products differ from their global counterparts as they are specifically derived to accurately reflect the bio-optical characteristics of each basin (e.g., Szeto et al., 2011; Volpe et al., 2007; Pitarch et al., 2016; D'Alimonte and Zibordi, 2003). Due to peculiarities in the optical properties, the Mediterranean Sea oligotrophic waters are less blue (30 %) and greener (15 %) than the global ocean (Volpe et al., 2007), causing an overestimation of the phytoplankton chlorophyll concentration

5 **(Chl)** retrievals by standard global algorithms (e.g. Bricaud et al., 2002, D'Ortenzio et al., 2002). In the last decade, more accurate regional bio-optical algorithms (e.g., MedOC4) were implemented in the single-sensor operational processing chains for the Mediterranean Sea (Santoleri et al., 2008; Volpe et al., 2012).

The main objective of this work is to provide Copernicus users with a comprehensive description of the method currently applied by GOS (the group for Global Ocean Satellite monitoring and marine ecosystem study, of the Italian National

10 Research Council, CNR) in the OCTAC context of CMEMS to produce the L3 multi-sensor ocean colour product over the Mediterranean Sea. Next section (Data and Methods) describes the bio-optical dataset forming the basis for the development and validation of the regional algorithms for the Mediterranean Sea, an update of the MedOC4 parameterization, as well as the satellite data input and output of the operational processing chain. Section 3 gives an overview of the validation results obtained in the comparison between the multi-sensor satellite products and the in situ data.

15 2 Data and Methods

2.1 The Mediterranean Sea in situ bio-optical dataset: MedBiOp

The development of geophysical products that best reproduce the Mediterranean biogeochemical conditions relies on **an** in situ bio-optical dataset collected across the basin over twenty years (Figure 1). Several parameters are routinely measured both for general oceanographic purposes (e.g., water temperature, salinity, **oxygen** content, fluorescence and light 20 attenuation) and for the calibration and validation of remote sensing data. **These** include phytoplankton pigment concentration via HPLC **analysis** (High Performance Liquid Chromatography), light absorption due to coloured dissolved organic matter (CDOM), **light absorption due** to algal and non algal particles as well as to total suspended matter (TSM), particulate back scattering and apparent optical properties such as **remote sensing reflectance** (Rrs) and the diffuse attenuation coefficient (K_d). In this work, the in situ Rrs dataset is used as input to update the MedOC4 Chl algorithm and to validate the multi-sensor satellite-derived Rrs product. The in situ Chl dataset is larger than the Rrs and all samples in correspondence of optical measurements are used to update the MedOC4 Chl algorithm, while all others are used to validate the multi-sensor satellite-derived Chl product. On the other hand, K_d measurements are only used to fine-tune the Mediterranean algorithm for ocean colour retrieval.

In the OC processing chain the primary parameters used to derive the geophysical products is the spectral Rrs. The most 30 important objective of using the **in situ** radiometric measurements is to derive surface, above-water Rrs spectra from in-water profiles. The multispectral Satlantic profiling system (OCR-507) is made for measuring the upwelling radiance, $L_u(z, \lambda)$, the downward and the upward irradiance, $E_d(z, \lambda)$ and $E_u(z, \lambda)$, and includes a reference sensor for the downward irradiance,

Deleted: CHL

Deleted: This work describes the main processing steps, the validation framework and results for the multi-sensor L3 product for the Mediterranean Sea, operationally performed within CMEMS by the Group for Global Ocean Satellite monitoring and marine ecosystem study (GOS) in Rome, Italy.

Deleted: The section Results and Discussion

Deleted: In Conclusions section we discuss the most important achievements with relevant concluding remarks and provide future perspectives.

Deleted: the

Deleted: Figure 1

Deleted: O

Deleted: , which

Deleted: both inherent and

Deleted: R

Deleted: S

Deleted: R

Deleted: In this work, in situ Rrs and Chl are used for both updating the MedOC4 Chl algorithm and for validating the multi-sensor satellite-derived Rrs and Chl.

Deleted: Remote Sensing Reflectance (

Deleted:)

Deleted: Here, t

Deleted: remote sensing Reflectance (

Deleted:)

Deleted: t

$Es(0,\lambda)$, mounted on the uppermost deck of the ship. A Sea-bird CTD and a tilt sensor are also part of the system. The radiometric measurements are acquired and processed following the method described in Zibordi et al. (2011). To increase the number of samples per unit depth, data are acquired using the multicast technique (D'Alimonte et al., 2010; Zibordi et al., 2004).

5 Multi-level data processing is achieved using the Software for the Elaboration of Radiometer Data Acquisitions (SERDA), developed at GOS. The processing steps follow the consolidated protocols for data reduction of in-water radiometry (Mueller and Austin, 1995; Zibordi et al., 2011). First, data are converted from digital counts into their physical units. A filter is applied to remove data with profiler tilt angle larger than 5° . In order to reduce the influence of the light variability during the measurements, data from each sensor are normalised by the above-water downwelling irradiance. A least-square linear regression is performed on the log-transformed normalised data, whose slope determines the diffuse attenuation coefficients of spectral upwelling Radiance ($Kl(\lambda)$), spectral upwelling Irradiance ($Ku(\lambda)$) and spectral downwelling Irradiance ($Kd(\lambda)$). the exponents of the intercepts are the sub-surface quantities ($Lu(0^-, \lambda)$, $Eu(0^-, \lambda)$ and $Ed(0^-, \lambda)$). Outliers due to wave perturbations are removed and identified in those points differing, by default, more than two standard deviations from the regression line. The depth layer normally considered as relevant for the extrapolation to the surface is 10 0.3-3 m, but can be changed on the basis of the characteristics of each profile. The upwelling sub-surface quantities (i.e. $Lu(0^-, \lambda)$, $Eu(0^-, \lambda)$) are also corrected for the self-shading effect following Zibordi and Ferrari (1995) and Mueller and Austin (1995) using the ratio between diffuse and direct atmospheric irradiance, and the sea-water absorption. Using the primary sub-surface quantities, it is then possible to derive additional products such as the Q-factor at nadir ($Qn(0^-, \lambda) = Eu(0^-, \lambda)/Lu(0^-, \lambda)$), the remote sensing reflectance ($Rrs(\lambda) = 0.543 \cdot Lu(0^-, \lambda)/Es(0, \lambda)$) or the normalized water-leaving radiance ($Lwn(\lambda) = Rrs(\lambda) \cdot E0(\lambda)$ with $E0(\lambda)$ being the extra-atmospheric solar irradiance; Thuillier et al., 2003).

Fluorimetric measurements associated with CTD casts are used to increase the depth resolution of the HPLC-derived chlorophyll. These calibrated fluorimetric casts are then used to compute the optically weighted pigment concentration (OWP) as already reported in Volpe et al. (2007).

In addition to the MedBiOp dataset collected by GOS over the Mediterranean Sea, two fully independent datasets, collected 25 at fixed location, are included for the validation in this study: Rrs data estimated from above-water measurements at the Aqua Alta Oceanographic Tower (AAOT) as part of the AERONET-OC network in the northern Adriatic Sea (Zibordi et al., 2009), as well as Rrs data from the BOUSSOLE buoy located in the Ligurian Sea (Antoine et al., 2008; Valente et al., 2016). Moreover, for the validation of the diffuse attenuation coefficient we use the independent BGC-Argo float dataset from Organelli et al. (2016).

30 2.2 Satellite Data Processing Chain

As mentioned, GOS operates two different processing chains (Figure 2), for the NRT/DT and for the REP data production. The input of both processing chains is the spectral Rrs downloaded from upstream data providers. Hence, in both cases, the atmospheric correction is not part of these processing chains. This approach differs from the previous regional processing

Deleted: In order t

Deleted:).

Deleted: Data

Deleted: Multi-level

Deleted: software for

Deleted: s

Deleted: Data

Deleted: MERDA

Deleted: t

Deleted: in

Deleted: with

Deleted:

Deleted: and t

Deleted:

Deleted: and Chl

Deleted: 7

Deleted: Figure 2

Deleted: near-real time

Deleted: reprocessed

Deleted: , respectively

Deleted: , e.g., the space agencies

chains which started from L1 (Volpe et al., 2007; 2012), as updates by the space agencies in the L1 to L2 processor resulted in a delay of months before it could be taken up in the operational processing chain.

As schematically shown in [Figure 2](#), the NRT/DT chain consists of four parts aimed at populating a two-year rolling archive with multi-sensor Level-3 data at daily temporal resolution. The rolling archive includes the L3 obtained by the NRT L2 data

5 (i.e., processed by with preliminary ancillary data, calibration known at the time of acquisition, preliminary climatology and so on), which are superseded, generally after one month, by the L3 produced in DT mode. Thus, the processing chain is exactly the same for the two modes, NRT and DT, what changes are the input data from space agencies. Data in the rolling archive are homogeneous in terms of format and processing software, meaning that if, for any reason, a change is made on the processing chain, the entire rolling archive is processed back for consistency. [The ingested L2 data \(R2018.0\) currently](#)
10 derive from MODIS-AQUA and VIIRS sensors only. L2 are downloaded from the Ocean Biology Processing Group (OBPG) at NASA which use the l2gen processor for the atmospheric correction in its default parameterisation (Mobley et al., 2016). The NRT/DT chain involves the pre-processing of different sensors with different wavelengths (as detailed in [Section 2.2.1](#)) that are then merged together over a common set of wavelengths ([Table 1](#), [Section 2.2.2](#)). [Section 2.2.3](#) provides a description of the algorithms for the satellite-derived Chl estimation and for the attenuation coefficient of light at
15 490 nm ([Kd490](#)). As it will be detailed later, the inherent optical properties (IOPs: the absorption due to phytoplankton, a_{ph} , and to detrital and dissolved matter, a_{dg} , and the backscattering due to particles, b_{bp} , all at 443 nm) are used to align the different sensors over the common set of wavelengths. For this reason, the IOPs are an active part of the processing and are also made available to users as output of the chain.

For the REP processing, Rrs spectra [over the common set of wavelengths \(Table 1\)](#) are produced by the Plymouth Marine
20 Laboratory (PML) using the OC-CCI processor version 3 (hereafter CCIv3, [www.esa-oceancolour-cci.org](#)) merging MERIS, MODIS-AQUA, SeaWiFS and VIIRS data. [As fully detailed in CCI \(2016a\)](#), SeaWiFS and VIIRS derive from the OBPG chain using the l2gen processor, while MERIS and MODIS-AQUA are processed with the POLYMER atmospheric correction processor (Steinmetz et al., 2011). At the moment of writing, the CCIv3 is based on the NASA reprocessing R2014.0. Within CMEMS, PML runs the regional CCIv3 processor at 1km resolution rather than at 4km as for the global
25 OC-CCI dataset. In the following of this work, with CCIv3 we will refer to both the processor and the derived Rrs exclusively made for CMEMS, whereas with REP we will refer to the output of this chain. Chl and Kd490. These are consistently retrieved with the same algorithms as in the NRT/DT chain ([Section 2.2.3](#)), updated on a yearly basis and are available to users on the CMEMS web portal ([marine.copernicus.eu](#)).

As shown in [Figure 1](#), most of the in situ data used for the validation analyses do not overlap with the two-year rolling
30 archive (2017-2018, at the time of writing). Hence, for the sole scope of the product validation, the NRT/DT production chain was used to process the entire satellite data archive, including SeaWiFS and MERIS data. SeaWiFS data were obtained from NASA-OBPG (R2018.0), while MERIS data are the ESA third reprocessing with the POLYMER, made available by PML.

Deleted: Figure 2

Deleted: .

Deleted: These d

Deleted: REF

Deleted: This

Deleted: Single sensor pre-processing s

Deleted: Table 1

Deleted: s

Deleted: Multi sensor processing: Rrs spectra

Deleted: The Level-3 geophysical products s

Deleted: derivation

Deleted: of Chlorophyll Concentration (Chl, in units of mg m⁻³)

Deleted: of

Deleted: Kd490

Deleted: , in units of m⁻¹

Deleted: are already available

Deleted: Table 1

Deleted: at those wavebands,

Deleted: A

Deleted: s fully detailed in [Melin E JACSON](#)

Deleted: (REF)

Deleted: as the entire data time series is processed with a consistent configuration, providing users with the longest and most consistent available data time series, spanning over twenty years (1997 to 2017), for the Mediterranean Sea. Within CMEMS, the spectral Rrs is produced by the Plymouth Marine Laboratory (PML), which uses the OC-CCI processor version 3 ([www.esa-oceancolour-cci.org](#)) to merge at 1km resolution (rather than at 4km as for OC-CCI) MERIS, MODIS-AQUA, SeaWiFS and VIIRS data; this dataset is hereafter referred to as CCIv3. At the moment of writing, the CCIv3 is based on the NASA reprocessing 2014.0. These data are updated on a yearly basis and are available to users on the CMEMS web portal ([marine.copernicus.eu](#)). The outputs of the

Moved down [7]: These data are updated on a yearly basis and are available to users on the CMEMS web portal ([marine.copernicus.eu](#)).

Deleted: chain are

Deleted: Kd490

Deleted: .

Deleted: These data are

Moved (insertion) [7]

Deleted: Figure 1

2.2.1 NRT/DT single sensor pre-processing

Once downloaded and quality checked, single-sensor L2 data are fed into the pre-processing chain to harmonize data from different sensors in terms of format, projection, and most of all in terms of a common set of wavelength bands. The quality checks that are operationally performed soon after the download are associated with the integrity of data files or their effective coverage over the region of interest (the Mediterranean Sea, in this case).

Moreover, the pre-processing also takes care of sorting out issues that may affect one sensor only such as the desstriping procedure or the removal of the bowtie effect.

Desstriping

An important task, operationally performed over both MODIS-AQUA and NPP-VIIRS images is the application of a desstriping procedure over L2 products to remove the instrument-induced stripes. These two sensors scan the Earth surface via a rotating mirror system that reflects the surface radiance to band detectors. Stripes originate from two hardware problems: i) the two sides of the mirror are not exactly identical, and ii) the band detector degradation is not homogeneous. Desstriping correction is performed by applying the method developed by Bouali and Ignatov (2014) and adapted to ocean colour products by Mikels ons et al. (2014). The procedure splits the image into a stripe-affected and a stripe-free part. The stripe-affected part is then passed through a filter that removes the stripes, and then is added back to the stripe-free component to produce the final desstriped image. The definition of striped and de-striped domains is achieved by measuring the gradients (both along and across the scan) and by selecting as “stripped” the ones below the pre-determined threshold values.

Removal of the bowtie effect

As sensor detectors have constant angular resolution, the sampled Earth area, i.e. the dimension of the pixel at ground, increases with the scan angle. This results in consecutive scans to overlap away from nadir, in turn giving the entire scan the shape of a bowtie. Differently than other sensors such as MODIS-AQUA, the aggregation scheme on board VIIRS removes this effect through a combination of aggregation and deletion of overlapping pixels, resulting in a series of rows of missing values at the edge of each L2 granule. These lines can be identified through the bowtie removal flag (BOWTIEDEL). In this production chain and in view of the sensor merging, these missing values are filled in by linear interpolation. Alas, the L2 flags associated with these pixels are not updated due to the difficulty of interpolating binary fields.

Flagging & Mosaicking

Each L2 granule is quality checked via the application of the L2 flags provided by Space Agencies. The L2 flags result from the atmospheric correction procedure and provide the sensing conditions at pixel scale. The flags currently applied are those of the OBPG standard processing (<https://oceancolor.gsfc.nasa.gov/atbd/ocl2flags/>), except for the atmospheric correction failure (ATMFAIL) flag that is not applied to VIIRS because it overlaps for almost all water pixels over the Mediterranean Sea with the BOWTIEDEL, thus effectively thwarting the interpolation of the lines affected by the bowtie effect. From a test over 645 granules (3200 x 3232 pixels each) acquired over the Mediterranean Sea in 100 days (10 April 2018 to 18 July

Deleted: For consistency, the wavelengths at which the Rrs spectra are provided to users are the same for both processing chains (REP and NRT/DT). Similarly, for compatibility, the same Chl and Kd490 algorithms are used in both processing chains (section Level-3 geophysical products).⁴

Deleted: (R2018.0 for SeaWiFS, MODIS-AQUA and VIIRS; third reprocessing for MERIS)

Deleted: which

Deleted: derive

Deleted: striped

Deleted: component

Deleted: component

Deleted: d component

Deleted: to

Deleted: eliminate

Moved down [2]: VIIRS data suffer of the bowtie effect.

Deleted: VIIRS data suffer of the bowtie effect. Sensor VIIRS_d[1]

Deleted: so that

Moved (insertion) [2]

Deleted: data suffer of the bowtie effect. The processing performed by space agencies generally

Deleted: in each VIIRS granule

Deleted: to both MODIS and VIIRS

Deleted: standard

Deleted: from space agencies

Deleted:

Deleted: for avoiding too many false positive pixels to be rejected

2018) it was found that only in 31 pixels the atmospheric correction failure flag was raised for pixels not affected by bow tie deletion or any of the other OBPG standard flags.

Moreover, each granule undergoes a further quality check by removing all isolated pixels (defined as those pixels with a meaningful value that are entirely surrounded by pixels with missing value) and by filling in all isolated missing pixels

Deleted: to remove the “salt and pepper” effect,

Deleted:

5 (defined as those pixels with the missing value that are entirely surrounded by pixels with a meaningful value) using the near-neighbourhood approach. All Rrs spectra are further checked for the presence of negative values, which may occur in the blue part of the spectrum due to the failure of the atmospheric correction; one negative value within the spectrum (excluding the 670nm band) is enough for the entire spectrum to be rejected. All available granules for each day are remapped at 1 km resolution on the Equirectangular grid covering the Mediterranean Sea (6°W-36.5°E, 30°N-46°N). All re-
10 gridded granules from the same sensor and from the same day are mosaicked together into a single file containing the Remote Sensing Reflectance at nominal sensors’ wavelengths.

Deleted: NIR

Deleted: s

Band-shifting
At the scale of the pixel, the goal is to merge single-sensor Rrs spectra into a single spectrum. The idea is that from the Rrs spectrum one can easily derive, directly or indirectly, all the geophysical parameters of interest not only for the ocean colour 15 community, but also for the wider biogeochemical scientific community. One of the problems of the multi-sensor merging is the different set of bands of the various ocean colour sensors that have to be merged. Some bands are coincident (443 nm), others may differ by a few nanometres (486 and 488 or 410 and 412 nm) while others can be significantly different (e.g., the green bands of MODIS-Aqua, SeaWiFS and OLCI, which are 547nm, 555nm and 560 nm respectively, [Table 1](#)). A technique to collapse the various spectra on a pre-defined set of bands is thus essential for the multi-sensor merging; to this
20 aim the band shifting method described by [Mélin and Sclep \(2015\)](#) was implemented here with the application of the Quasi Analytical Algorithm (QAA version 6, Lee et al., 2002 and following updates http://www.ioccg.org/groups/Software_OCA/QAA_v6_2014209.pdf) in forward and backward modes. Rrs is related to the absorption and scattering properties of the medium, which in turn are given by the additional contributions of all the medium components (seawater, particulate and dissolved matters). Starting from the Rrs at the sensor native wavelengths and from
25 the characteristic spectral shapes of the IOPs, the QAA allows the estimation of the IOPs at target wavelengths. The QAA is then applied in forward mode to estimate the Rrs at these bands. The accuracy of QAA retrievals over the Mediterranean Sea was assessed with a limited number of observations by Pitarch et al (2016), who found that b_{555} at 555 nm was retrieved within 5% of [in situ measurements across open and coastal waters](#). This approach produces a set of common bands (grey-shaded in [Table 1](#)) for all sensors and allows the daily merging of the Rrs from which it is then possible to apply algorithms
30 to derive geophysical products. The uncertainty introduced by band shifting is estimated in most cases at well below 5% of the reflectance value (with averages of typically 1–2%), especially for open ocean regions (Mélin and Sclep, 2015).

Deleted: of

Deleted: Table 1

Deleted: Mélin

Deleted: In general,

Deleted: (5

Deleted:)

Deleted: i

Deleted: Table 1

Deleted: , in theory,

Deleted:

Deleted: the

Deleted: the

2.2.2 NRT/DT multi sensor processing: Rrs spectra

Once single sensor spectra are homogeneous in terms of wavebands, it is possible for the Rrs from the available sensors to be merged together into single images. The output is a set of six Rrs images, each of which is treated as an individual image independently from the other Rrs bands of the spectrum.

5 Differences between MODIS and VIIRS

At pixel scale, several reasons can be at the base of the differences between two observations. The geometry of the observations constitutes an issue that is under the control of the atmospheric correction scheme. Since this part of the processing is performed by space agencies, this issue is rarely accounted for in the context of L3 multi-sensor merging, which instead only considers the radiometric quantities as fully normalized (Maritorena and Siegel, 2005). The order of

10 magnitude difference between Rrs retrieved by MODIS and VIIRS varies with the wavelength (Figure S.1). The distribution of the Rrs ratio at 670 nm shows the most negative kurtosis. At 412 nm, the median Rrs ratio ranges between 0.7 and 1, while at 443 it improves and narrows to 0.85 and 1.05, with MODIS being in general below VIIRS. For the three other bands (490, 510 and 555 nm), the Rrs ratio distribution displays the narrowest spread around 1, with the median values ranging between 0.9 to 1.1. Moreover, a pixel is sampled with different geometry (scattering angle) and not exactly at the same time

15 by the two sensors; in the Mediterranean Sea, the differences between the two sensor time overpasses do not exceed one hour. Here, we tested that the discrepancy between the two Rrs spectra cannot be ascribed to differences in the overpass times and/or to the geometry of the observation (Figure S.1). We argue that there must be other factors responsible of the observed differences such as inter-sensor calibration or even the various bands used for operating the single-sensor atmospheric correction (eliciting different responses by the atmospheric correction code and its assumptions/simplifications).

20 All these issues should be addressed before any sensor merging can effectively be performed (Sathyendranath et al., 2017).

Inter-Sensor Bias Correction

Before merging all the available sensors together at any given time, their Rrs spectra are individually bias-corrected with respect to their references as detailed below. Here, we extend the method developed within OC-CCI for reducing the inter-sensor bias (CCI, 2016b), as this is a propedeutical step to the proper merging of data collected from different sensors. In

25 practice, when two or more sensors are available for the same period, one sensor is taken as reference and the others are bias-corrected to the reference. For the inter-sensor bias to be corrected, daily climatological bias maps are computed at the same spatial resolution of the source data (e.g., 1 km). During the SeaWiFS era, the method is applied to SeaWiFS-MODIS-MERIS sensors having SeaWiFS as reference. From 2010 onward, the method is applied to the couple MODIS-VIIRS using MODIS as reference, after its bias with SeaWiFS is corrected. The climatological bias maps were computed using data from

30 2003 to 2007 for the SeaWiFS era, and from 2012 to 2014 for the other.

Briefly, the OC-CCI scheme to compute the daily climatological bias maps is:

- 1) over the periods of reference, for each sensor, a rolling temporary daily average map of Rrs is computed (simple mean) over the period of 7 days: the data day itself plus 3 days before and 3 days after.

Deleted: Multi

Deleted: In other words, we move from the wavelength domain in which each pixel is associated with a common set of Rrs bands (a spectrum), to the spatial domain in which the aim is to assign a value to all pixels that were validly sampled, independently from the sensor that actually acquired the observation.

Deleted: is approximately 10%, although not uniformly distributed through the entire visible spectrum, and

Deleted: above

Deleted: Rrs a

Deleted: t

Deleted: nm

Deleted:

Deleted: the line of best agreement and lower than

Deleted: 10%

Deleted:, whereas other bands show wider distribution reaching values of about 15% difference (data not shown)

Deleted:

Deleted: .

Deleted: approximately 10%

Deleted: difference

Deleted:, and that

Deleted: it

Deleted: due to

Deleted: issues which must be addressed before any sensor merging can effectively be performed (Sathyendranath et al., 2017)

Moved (insertion) [6]

Deleted: ,

Deleted: must

Moved up [6]: which must be addressed before any sensor merging can effectively be performed (Sathyendranath et al., 2017)

Deleted: .

Deleted: by

Deleted: Melin et al. (2017)

- 2) For each day, the ratio between the temporary average Rrs maps from the various sensors is computed.
- 3) This allows the calculation of 365 daily climatology maps of the ratio between each pair of missions over the periods of reference.
- 4) To increase map coverage and to reduce the spatial gradients, smoothing of the daily climatology bias maps over a temporal window of $2N+1$ days (with $N=60$) are computed following equations 1 and 2:

$$\delta(d, x, y) = \frac{\sum_{i=-N}^N w_i \delta_i(d+i, x, y) \theta_i}{\sum_{i=-N}^N w_i \theta_i}, \quad (1)$$

5 with

$$w_i = \frac{N+1-|i|}{N+1}, \quad (2)$$

where $\delta(d, x, y)$ is the daily bias map climatology, and $\theta_i = 1$ if δ_i is associated with a valid value, zero otherwise. The value 10 of the weight w_i decreases from 1, for the same day, to $N/N+1$ for the days before and after, to $1/N+1$ for the first and last days of the $\pm N$ -day window.

The way the daily climatological bias maps are here computed differs from the OC-CCI technique. First, the rolling 15 temporary seven-day average (point 1 of the OC-CCI method described above) is here computed using equations 1 and 2, with $N=3$. The smoothing of the daily climatology bias maps is obtained by applying a weighting-function (as point 4 of the OC-CCI method described above) in both space and time, contemporaneously. The spatial kernel of the 3×3 box centred to the pixel is defined as:

0.25	0.50	0.25
0.50	1.00	0.50
0.25	0.50	0.25

The cumulative effect of these two weighting functions is given by their cross product.

Furthermore, the method was not applied to the 670 nm band because the percent difference between SeaWiFS and in situ 20 observations at 670 nm is one or two orders of magnitude larger than the blue-green counterparts in both oligo- and mesotrophic conditions (MedBiOp, BOUSSOLE) (Section 3). Moreover, the number of matchups between SeaWiFS and all the available in situ data (MedBiOp, BOUSSOLE and AAOT) at 670 nm is ~40% of those in the blue-green spectral region (data not shown).

Sensor-Merging

25 When merging data from two or more sensors, three possible conditions can occur: i) the pixel is observed from more than one sensor, ii) the pixel is observed from one sensor only, iii) the pixel is in no clear sky condition or masked out because of any of the operational L2 flags, from all sensors. In the latter case the pixel is assigned the missing value. In the former two conditions the merging is not straightforward because it strongly depends on the ability to reduce the inter-sensor bias to zero. When the pixel is sampled by one sensor only, but the surrounding pixels by more than one or by the other sensors, 30 there is an increasing probability of introducing artefacts or spatial gradients, which in reality do not exist and are only the

Deleted: 1

The equation for computing the daily climatology bias maps over the $2N+1$ days (with $N=60$) is

Moved (insertion) [3]

Deleted: of the climatology

Deleted: 0.75 (

Deleted:)

Deleted: 0.25 (

Deleted:)

Deleted: 3

Deleted: bias

Deleted: is

Deleted: in two steps: i)

Deleted: first

Deleted: from three days prior to three days after the day of interest

Deleted: ,

Moved up [3]: where $\delta(d, x, y)$ is the daily climatology, and $\theta_i = 1$ with a valid value, zero otherwise. The value of the weight decreases from 1, for the same day of the climatology, to $0.75 (N/N+1)$ for the days before and after, to $0.25 (1/N+1)$ for the first and last days of the ± 3 -day window.¹

As for the averaging method for computing the climatology map, we applied a weighting-function not only in the time dimension but in both space and time, contemporaneously. As for the OC-CCI, the time window is set to 60 days. The spatial kernel of the 3×3 box centred to the pixel is defined as:¹

Moved (insertion) [4]

Deleted: ii) the averaging method for estimating the climatology maps and iii) this method was not applied to the 670 nm band. The seven-day average is computed to enhance data coverage and, rather than a simple average, here it is derived using a weighted-averaging function that gives more importance to the data day with respect to those that are away from it. The equation for computing the daily climatology over the $2N+1$ days (with $N=3$) is:¹

$$\delta(d, x, y) = \frac{\sum_{i=-N}^N w_i \delta_i(d+i, x, y) \theta_i}{\sum_{i=-N}^N w_i \theta_i}, \quad (1) \quad \dots [2]$$

Deleted: Furthermore, as better detailed later,

Deleted: (

Deleted:)

Deleted: The cumulative effect of these two weighting functions^[3]

Deleted:

Moved up [4]: Furthermore, as better detailed later, the percent

Deleted: ¹ ... [4]

Deleted: method

Deleted: given by

result of the merging procedure. To prevent the occurrence of such horizontal discontinuities, here we apply a smoothing procedure based on the use of the climatology field, described in Volpe et al. (2018) and summarized below. First, the field from each sensor (Figure 3a-b) is filled with the same relevant daily climatology (Figure 3e, see below for more details about the climatology), as shown in Figure 3c-d. Filling is performed as follows: for each sensor, the difference between the two fields (observed and climatology) is first computed in correspondence of co-existing values. Such difference is propagated and smoothed all over the spatial domain. Missing observational values are replaced with the climatology corrected by the computed difference map. This prevents the generation of sharp gradients. At this stage, the simple average between all available climatology-filled sensor data is computed. Then all the non-clear sky pixels are set to the missing value (Figure 3f). This is the procedure operationally and currently applied to data acquired by MODIS-AQUA and VIIRS to produce the multi-sensor Rrs product. It is important to note that features, which are only present in the climatology, but not in the daily single-sensor images, are also absent in the merged product. In the example of Figure 3, features of such a kind can be clearly identified in correspondence of the Strait of Bonifacio, in the Tyrrhenian Sea, which extends eastwards only in the climatology (Figure 3e) but in none of the other fields (MODIS-AQUA or VIIRS). Another example is given by the tongue of Modified Atlantic Water (Manzella et al., 1990) that penetrates the southern sector of the Sicily Channel towards the Libyan coasts, which is present in AQUA, VIIRS, and in the merged image, but not in the climatology. Similarly, the Rhone River plume, visible in the climatology as a small reddish spot, is absent from both single-sensor images and from the merged multi-sensor product.

After all bands are merged, single pixel Rrs spectra are available (Figure 4) for the geophysical products to be computed. Within this step, a mask is computed for keeping track of the single sensor inputs to the multi-sensor product and added to the NetCDF files (Figure 4b and Figure 4d). The examples show two cases of blue and greener waters along the Spanish coast and in the northern Adriatic Sea, respectively. In both cases, the bias correction demonstrates to improve the satellite Rrs estimate being closer to the in situ measurements, at all bands.

Climatology

As mentioned the climatology provides a spatial support to the sensor merging. The climatology field is obtained from the thirteen years of SeaWiFS data. This daily field has the same spatial resolution (nominally 1 km at nadir) and projection (cylindrical) as the operational field. These climatology maps were created using the data falling into a moving temporal window of ± 5 days. Five days are deemed to be a good compromise between the need of filling the spatial domain and the de-correlation time scale of the OC data in the Mediterranean Sea; this has been estimated as being 3 days on average (the day at which the autocorrelation value halves, Volpe et al., 2018). The resulting daily climatology time series includes the pixel-scale standard deviation, the average, the median, the modal, the minimum, and the maximum values. The next version of the NRT/DT processing chain will include a climatology field computed by taking into account the space-time weighted averaging and a longer and more recent data time series.

Deleted: the

Deleted: described in Volpe et al. (2018)

Deleted: Figure 3

Deleted: Figure 3

Deleted: Figure 3

Deleted: This enables the average of these two (or more) fields to be easily computed. A

Deleted: observed

Deleted: then

Deleted: Figure 3

Deleted: Figure 3

Deleted: to

Deleted: the west coast of Italy

Deleted: Figure 3

Deleted: Figure 4

Deleted: Figure 4

Deleted: Figure 4

Deleted: using the MedOC4 regional algorithm for CHL (Volpe et al., 2007)

Deleted: One of the main purposes of a climatology field is to serve as reference, and as such it is expected to be as reliable as possible, thus avoiding biases caused by single incorrect pixel values. To overcome these possible biases, a filtering procedure is applied to the entire SeaWiFS time series, by removing all isolated pixels and by filling in all isolated missing pixels using the near-neighbourhood approach.

2.2.3 Level-3 geophysical products

The input to all algorithms used to derive the various geophysical products is the Rrs spectrum, which in this context derives from the NRT/DT processing chain described above and from the CCIV3 processor. It should be noted that in the L1 to L2 processing performed by the space agencies, the water leaving radiance normalization scheme makes use of Chl values

5 estimated with standard algorithms. The differences between standard Chl and MedOC4 estimates in the Mediterranean Sea might affect the accuracy of the resulting Rrs. However, in the context of L3 multi-sensor merging this inconsistency cannot be accounted for without performing the L1 to L2 processing in house. The previous regional processing chains started from L1 and did take this effect into account (Volpe et al., 2007; 2012). On the other hand, in the operational oceanography framework, the need to keep the L2 to L3 processing chain readily up-to-date imposes a trade-off between accuracy and

10 timeliness.

As shown in Figure 2, from this point on, the NRT/DT and the REP chains collapse as they both use the same algorithms for computing Chl, Kd and the IOPs. Next sections explain how the various algorithms are derived and applied to Rrs data for their operational application.

Chlorophyll a concentration

15 There are two main categories of Chl algorithms, empirical and semi-analytical. Even though the latter now show performance comparable to that of empirical algorithms, these still remain more robust and are generally preferred in the operational context (e.g., NASA processing). Recently, Sathyendranath et al. (2017) discussed the characteristics that remote sensing data must have to be used in climate studies. They pointed out that semi-analytical algorithms would be preferred to empirical ones because they do not rely on past observations, which are not necessarily the best approximation for future 20 observations (Dierssen, 2010). However, they still lack the robustness, which is typical of the empirical family of algorithms (O'Reilly et al., 2000 among others).

Operational services such as CMEMS aim at providing data for a wide range of applications from the assimilation of open 25 ocean observations into biogeochemical models (Teruzzi et al., 2014) to coastal monitoring programs (such as the Marine Strategy Framework Directive, e.g. Colella et al., 2016). Unfortunately, there is not yet a unique Chl algorithm able to

perform with the same accuracy across different environments. For example open ocean waters are prevalently dominated by phytoplankton cells and their products of degradation; these waters are well represented by chlorophyll concentration and are generally referred to as Case I waters (Morel and Prieur, 1977). On the other hand, the optical properties of coastal regions are more often influenced by various water constituents not necessarily covarying with phytoplankton and are referred to as Case II waters. Since the offshore extension of the coastal waters may vary and be of several kilometres (pixels), depending

30 on the sea and weather conditions (e.g., coastal filaments may extend several tens of kilometres in the open ocean), the adoption of static masks for the application of different algorithms would result in errors associated with the sharp fronts. One way to overcome this issue is to merge two Chl products into a single field, after the exact identification of the two realms (Mélin et al., 2011; Volpe et al. 2012; Moore et al., 2014). At pixel scale, Rrs spectra are translated into Chl twice:

Deleted: The first output of the processing chain is the Rrs spectrum derived from the method described above, and that constitutes the input to all algorithms used to derive the various geophysical products.

Moved (insertion) [8]

Deleted: ↗

Deleted: Figure 2

Deleted: Despite the latters became mature enough to be often compared to the performances of the empirical algorithms

Deleted: in the context of what are the best characteristics that data must have to be used

Deleted: ,

Deleted: Sathyendranath et al. (2017)

Deleted: , despite

Deleted: theoretical

Deleted: (semi-analytical) are

Deleted: (they

Deleted: , as shown in

Deleted:),

Deleted: OC4-

Deleted: water types.

Deleted: whether

assuming the entire satellite scene to belong to Case I and to Case II waters, each with its own algorithm. Then, the water type identification follows the method developed by D'Alimonte et al. (2003) which uses the Mahalanobis distance between the satellite spectrum and the in situ reference spectra (in terms of the mean values and the covariance matrices of the two experimental datasets). For Case I and Case II waters the MedOC4 (Volpe et al., 2007) and CoASTS (Berthon et al., 2002,

5 Zibordi et al., 2002) datasets are used, respectively. This approach is one step towards the need of the scientific community of dealing with products performing equally well in both water types, or at least to know where the first ends and the second starts (Sathyendranath, 2011, OC-CCI user consultation). To address also the latter point evidenced by the OC-CCI user 10 consultation, a water type mask resulting from the Case I-Case II merging step is conveniently stored into the NetCDF files and made available to users. Thus two different algorithms are used to derive Chl in the two optical domains: the ADOC4 algorithm (D'Alimonte and Zibordi, 2003) is used for the Case II domain, while algorithm for Case I constitutes the matter of the next paragraph.

Mediterranean Sea – MedOC4 – Case I

The algorithm used to retrieve Chl in the Case I waters of the Mediterranean Sea is an updated version of the MedOC4, a regionally parameterized Maximum Band Ratio (Volpe et al., 2007). Figure 5a shows both the regional and the global

15 algorithm (OC4v6, https://oceancolor.gsfc.nasa.gov/atbd/chlor_a/) functional forms superimposed to the in situ observations collected in the Mediterranean Sea. The Mediterranean Sea tends to be “greener” than the Pacific and Atlantic oceans for any Chl values due to higher CDOM concentrations (Volpe et al., 2007 and references therein). Considering that the empirical 20 algorithms are the expression of the in situ data from which they are derived, this figure provides a means for understanding the need to regionalize the algorithms to avoid the significant Chl overestimation that would be obtained with the global algorithm, as already fully documented in Volpe et al. (2007, and references therein).

An important point that has to be borne in mind is that the colour of the ocean, in terms of maximum band ratio (MBR), explains 74% of the entire phytoplankton variability, as expressed by the determination coefficient (r^2) between the chlorophyll concentration and MBR (Figure 5a). This points to the importance (more than 25%) of the second order variability of the ocean colour signal (Brown et al., 2008) that should be accounted for by future versions of the operational 25 algorithms, in line with the recent recommendation about the use of ocean colour data for climate studies (Sathyendranath et al., 2017).

Diffuse Attenuation Coefficient - Kd490

Figure 5b (red dots) shows the in situ diffuse attenuation coefficient of light at 490 nm as a function of the Rrs ratio ($R = \log_{10}(Rrs490/Rrs555)$, collected in the Mediterranean Sea. Superimposed to the in situ dataset is also the algorithm 30 functional form (turquoise line) used in the OBPG processing at global scale (https://oceancolor.gsfc.nasa.gov/atbd/kd_490/). It is clear that the global algorithm only marginally overlaps with the in situ data, thus prompting for a regional dedicated algorithm to be developed. Black line is the in situ data best fit computed as a fourth power polynomial expression of the Rrs ratio, whose functional form is applied to the Multi Rrs ratio.

Deleted: Then, to identify the pixels belonging to Case I and Case II conditions, the identification of the two water types relies on the in situ reference Rrs spectra as fully described in D'Alimonte et al. (2003). For the computation of these two average spectra two distinct datasets were used;

Deleted: for

Deleted: survey

Deleted: Figure 5

Deleted: CHL

Deleted: 20

Deleted: Kd490

Moved (insertion) [10]

Deleted: Figure 5

Deleted: both

Deleted: regional and the global algorithm functional forms superimposed to the in situ observations

Deleted: The algorithm used to compute the diffuse attenuation coefficient of light at 490 nm is

Moved up [10]: Figure 5b shows both the regional and the global algorithm functional forms superimposed to the in situ observations collected in the Mediterranean Sea.

Deleted: ($R = Rrs490/Rrs555$)

Deleted: as already done at global scale (https://oceancolor.gsfc.nasa.gov/atbd/kd_490/)

Deleted: A subset of the in situ bio-optical dataset used for Chl is used to compute the algorithm for the retrieval of Kd490.

Deleted: All the available Kd490 observations from the CNR in situ dataset were used for the development of the algorithm so that we are unable of performing an independent validation.

2.3 Validation framework

The validation of the satellite products was carried out by pairwise comparison with the in situ observations: Chl and apparent optical properties, e.g., kd490 and Rrs. For determining co-location between in situ and satellite data records all measurements acquired in the same day were used, as L3 data used in this study do not preserve the time information. Then,

5 similarly to Zibordi et al. (2012), the median values is extracted from a 3 by 3 box centred on the in situ measurement coordinates, only if at least 5 pixels have valid values and the coefficient of variation is smaller than 20%. Bailey and Werdell (2006) use narrow time window for determining coincidence (i.e. no more than ± 3 h); Figure S.2 presents the percent difference between satellite and in situ Rrs for time windows ranging between ± 1 and ± 8 hours, assuming 10 am UTC as satellite overpass time. The range of variability of the relative difference is always within 1%, confirming recent 10 results from Barnes et al. (2019).

The uncertainty associated with the in situ data is due to several factors, e.g., the sea conditions, the operator ability which in turn can introduce several contamination factors; hence, here we consider satellite and in situ observations to be both affected by uncertainties (Loew et al., 2017). Thus, for the matchup analysis, a type-2 regression (also called orthogonal regression) is implemented here (Laws and Archie, 1981). The statistical parameters for the assessment of satellite versus in 15 situ data are listed in Table 2. For log-normally distributed variables (such as Chl and kd490) both datasets are log-transformed prior to computing the slope (S), the intercept (I) and the determination coefficient. A good match between the two observations is achieved when S is close to one and I is close to zero. The RMSD is the average distance of a data point from the fitted line, measured perpendicular to the regression line. RMSD and bias have the same units as the data from which they are derived.

20 3 Results and Discussion

This section provides the validation analysis for the operational NRT/DT retrievals of Rrs and Chl with the multi-sensor merged approach. The NRT/DT products (Multi) are available in the CMEMS catalogue as a rolling archive spanning two years, prior which REP products are available instead. As already mentioned, since most of the in situ data used for the validation analyses were collected earlier than 2017 (two years ago, at the time of writing), we used the NRT/DT production 25 chain described in Section 2.2 to process the entire satellite data archive. The validation of the REP products based on the CCIv3 is also included for comparison.

Temporal trend

In this context and with the general aim of identifying any temporal dependence of the computed statistics, the analysis was made comparing the satellite products with space-time collocated in situ measurements for each campaign separately and for 30 the whole dataset. No significant temporal behaviour emerged from the analysis (results not shown), highlighting that both in situ and satellite data are homogeneous in time and well calibrated. Similar results were recently yielded at global scale by Sathyendranath et al. (2017).

Matchup – Rrs single-sensors, multi-sensor

Figure 6 shows the relative difference between satellite and the MedBiOp Rrs spectra. Satellite Rrs at all available bands for each sensor are compared with the same in situ Rrs bands (Table 1). In general, the Rrs in the blue bands (443 and 490 nm) performs better than those at 412 nm or those in the green region (510 and 555 nm). As mentioned above, SeaWiFS, MODIS-AQUA and VIIRS are all processed with the l2gen processor, so that it is not surprising that these three sensors display a common spectral behavior with respect to in situ observations. On the other hand, MERIS is the only one exhibiting a positive difference with respect to in situ observations for the 412 and 443 bands. This is likely due to the different processing (performed by ESA) for the L1 to L2 processing of MERIS (see section 2.2 for details). Apart from the 670 nm band (76%), SeaWiFS performs generally better than the other sensors, thus supporting the choice of being selected as reference sensor for the blue-green spectral range. All other satellite data never exceed 15% relative difference when compared with in situ observations at basin scale (Table S.2 to Table S.7). A noticeable feature presented in Figure 6 is the wide variability of the computed statistics (given by the standard deviation bars) highlighting that the satellite data presented here do not substantially differ from the in situ observations. Table 3 shows the full statistics for the Multi Rrs product. One of the main reasons for merging data from different sensors is to enhance the domain coverage by reducing the influence of both the cloud coverage and generally flagged or masked pixels as well as the out-of-satellite-swath areas; in all cases the use of a multi-sensor approach increases the probability of valid clear sky observations. Figure 7 shows the time series of the percent basin coverage for four single sensors (SeaWiFS, MERIS, MODIS-AQUA and VIIRS) and of the Multi product. The number of clear sky pixels of the Multi is on average larger than that of the single sensors by as much as 40% (Figure 7), with minimum impact during winter and maximum at summertime. The difference between periods of maxima and minima somehow reflects the cloud cover influence over the multi-sensor product, with the winter-time being characterized by both cloud-cover and out-of-satellite-swath, while the summer periods being mostly affected by out-of-satellite-swath masked areas. Moreover, the coverage is higher in the period 2002–2011 when SeaWiFS (until 2010), MODIS-AQUA and MERIS were operating simultaneously. Despite the loss in 2010 of SeaWiFS with its very wide swath, in the entire 2011 the gain (turquoise line in Figure 7) does not decrease substantially. After the loss of MERIS in 2012 the gain in the percent basin coverage dramatically decreases. Thus the basin coverage depends in first instance on the number of available sensors but also to the relationships of the orbital parameters among the various OC missions. Results in Figure 6 are representative of the performances of the various satellite observations (both single- and multi-sensors) against the in situ measurements that were widely collected over the basin in the past twenty years, the MedBiOp dataset. Similarly, Figure 8 shows the comparison of the two multi-sensor time series (Multi and CCIv3) against three in situ datasets: the basin scale dataset (MedBiOp) and two fixed location datasets (section 2.1), one of which coastal (AAOT). In general, one could expect the mismatch between satellite and in situ observations to be larger at the extreme bands of the spectrum, i.e., at 412 nm and 670 nm. In the first case, because of the spectral distance from the NIR bands used for the atmospheric correction, and in the second because of the generally very low Rrs values that pose a challenge for both in situ and satellite determination of the Rrs at this band. Here, the difference between satellite and in situ Rrs observations at these

Deleted: Figure 6

Deleted: Table 1

Deleted: There is a common spectral behaviour between satellite and in situ observations, with the Rrs in the blue bands (443 and 490 nm) performing better than those at 412 nm or those in the green region (510 and 555 nm).

Deleted: Rrs in the blue bands (443 and 490 nm) performs generally better than those at 412 nm or those in the green region (510 and 555 nm).

Deleted: 56

Deleted: Figure 6

Deleted: significantly

Deleted: Table 3

Deleted: Figure 7

Deleted: three

Deleted: MODIS-AQUA, VIIRS and

Deleted: multi

Deleted: -sensor

Deleted: each

Moved (insertion) [9]

Deleted:

Deleted: multi-sensor

Deleted: 20

Moved up [9]: by as much as 20%, with minimum impact during winter and maximum at summertime.

Deleted:, with a noticeable decrease since 2012 likely due to the similar orbit periods of MODIS-AQUA and VIIRS

Deleted: 1

Deleted: Figure 6

Deleted: Figure 8

Deleted: s

Deleted: CCIv3

Deleted:).

Deleted: :

Deleted: .

Deleted: The

extreme bands is of the same order of magnitude as the blue-green part of the spectrum when observed in open ocean (MedBiOp and BOUSSOLE) but not in the coastal domain (AAOT). CCIv3 and Multi Rrs present a general good agreement, differences being smaller than 5%; this low difference is likely due to the two source datasets which are derived from two different NASA reprocessings, R2014 and R2018; at 412 nm, and to a lesser extent at 443 nm, this difference is

more pronounced (more than 5%) because the impact of the R2018 is larger at these bands. An even more evident difference (larger than 10%) is evident at 670 nm; here the impact of R2018 should be less important than in the blue bands. One important difference between Multi and CCIv3 is that Multi is not bias-corrected over SeaWiFS at this band (section 2.2.2); since SeaWiFS performances at this band are not as good as at the other bands it is reasonable to assume that this might be the cause of the observed discrepancy, further supporting the choice of not using SeaWiFS to bias-correct the other sensors in this band. Another important feature in Figure 8 is the general difference of satellite performance (both Multi and CCIv3) in coastal and open waters. Statistics associated with the two open ocean datasets (MedBiOp and BOUSSOLE) are of the same order of magnitude and much better than those computed in the coastal domain (AAOT).

Table 4 shows the number of matchups for each band of Multi and CCIv3 in correspondence of the three in situ datasets. Two aspects emerge: one linked to the difference between Multi and CCIv3 and the other between the 670 nm band and the other bands. As mentioned earlier, it is reasonable to assume that the different source data (R2018.0 for Multi and R2014.0 for CCIv3) is responsible for the differences in spatial coverage and hence in the number of matchups. Moreover, it should be mentioned that MODIS-AQUA used in the Multi processing chain derives from NASA R2018.0, while it derives from POLYMER atmospheric correction scheme for CCIv3. As for the differences between the 670 nm band and the other bands, the very noisy spatial patterns present in the daily images of the Rrs at 670 nm very often result, at the scale of the matchup pixels, in the coefficient of variation to exceed the 20% threshold (section 2.3).

Overall, despite their absolute differences, the two multi-sensor satellite products show a similar level of accuracy which suggests that the Multi processor is also suitable for the REP processing chain. This would provide the two benefits of reducing the number of upstream data provider and of giving the NRT/DT and REP products full compatibility.

Matchup – Chl

Figure 9 shows the matchups for the L3 Chl product for both processing modes, REP (derived from the CCIv3 Rrs) and NRT/DT (derived from the multi-sensor merged described in this study). To facilitate the comparison between the two satellite products, the matchup dataset includes only the points in which both satellite data are available. Both products are regularly distributed around the line of best agreement for the entire Chl range, although for in situ values larger than 0.3 mg m⁻³ there is a noticeable dispersion increase. Table 5 shows the statistics of the four datasets plotted in Figure 9. To assess the uncertainties of the Multi Chl currently distributed on the CMEMS portal, the analysis was performed on the period in which VIIRS and MODIS co-exist, i.e. January 2012 onwards. Despite the different number of matchups (44 vs 710) and different Chl ranges (~0.04–2 vs ~0.007–9), statistics associated with the full time series are totally comparable with those obtained with the most recent data only (2012 to present) as denoted by the AV (MODIS-AQUA and VIIRS) subscript in both Figure 9 and Table 5.

Deleted:, while it appears significant relevant

Deleted: The use of the NASA reprocessing (R2018.0) in the Multi but not in the REP (CCIV3 which builds on R2014) is the likely cause for the different performances in the blue region.

Deleted:

Deleted: In the NIR 670 nm regionband, the spread of results between different satellite data among the three in situ reference observations is largest. One reason can be given by the less large difference in the

Deleted: used

Deleted: at 670 nm than at the other

Deleted: bands ((Table 4)

Deleted:) SPIEGARE IL PERCHE

Deleted:).

Deleted: the use of

Deleted: products

Moved up [8]: It should be noted that in the L1 to L2 processing performed by the space agencies, the water leaving radiance normalization scheme makes use of Chl values estimated with standard algorithms. The differences between standard Chl and MedOC4 estimates in the Mediterranean Sea might affect the accuracy of the resulting Rrs. However, in the context of L3 multi-sensor merging this inconsistency cannot be accounted for without performing the L1 to L2 processing in house. The previous regional processing chains started from L1 and did take this effect into account (Volpe et al., 2007; 2012). On the other hand, in the operational oceanography framework, the need to keep the L2 to L3 processing chain readily up-to-date imposes a trade-off between accuracy and timeliness.

Deleted: Figure 9

Deleted: Table 5

Deleted: Figure 9

Deleted: asses

Deleted: November

Deleted: 2011

Deleted: .

To further assess the level of accuracy associated with the Chl retrieval from multi mission merged approach presented in this study, we compared with the results at global scale reported in Climate Assessment Report, CAR, (CCI, 2017). Differently than here, in the CAR, the Chl log-transformation was used to compute all the statistics, not only those associated with the linear fit (slope, intercept and determination coefficient, section 2.3). Therefore, for this analysis, we recomputed all 5 the statistics of Table 5 accordingly (Table S.10). The in situ data used to compute the CAR statistics are much more numerous (14582, Table S.10). Nonetheless, results for the proposed regional algorithms as well as for CCI at global and Mediterranean scales show a general good agreement in terms of the determination coefficient, RMSD, CMRSD and the slope of the linear fit. The difference in the intercept only reflects the difference in the two dataset range of variability, with the global being wider and characterized by larger modal value (centred over $\sim 1 \text{ mg m}^{-3}$, Figure 8 in CAR) than the 10 MedBiOp (Figure 9).

Matchup – kd490

Figure 10a shows the validation result of the satellite-derived kd490 with respect to the in situ kd490 obtained from the BGC-Argo float dataset (Organelli et al., 2016). As a matter of comparison, both algorithms shown in section 2.2.3 and in Figure 5b are also presented. A general overestimation of the in situ kd490 is clearly visible in both the global and the 15 Medkd algorithms for kd490 values below 0.04 m^{-1} and 0.06 m^{-1} , respectively. Organelli et al. (2017) show analogous results with the satellite data overestimating the BGC-Argo – derived kd490 values below 0.1 m^{-1} (their Figure 11). Here, since the satellite kd490 are derived from the two algorithms applied to the Multi Rrs, the level of accuracy that one can expect should be of the same order of magnitude as the one shown in Figure 6 and Table S.7. However, statistics associated with this 20 matchup analysis show that both algorithms do perform worse than expected (Table S.9), especially the Medkd. There can be a series of reasons for which the two datasets (satellite and in situ) show good or bad agreement. One such a reason could be linked to the different space-time distribution of the calibration and validation datasets, but from the comparison of Figure 1 and Figure 10c it does not appear to be the case. The different data distribution can at least partially explain the poor performances of the Medkd with respect to the BGC-Argo kd490 (Figure 10b). As already mentioned in section 2.2.3, the Global algorithm appearing inadequate to represent the Mediterranean Sea conditions was superseded by the regional Medkd 25 algorithm. The fact that in the validation exercise, the Global algorithm performs better than the Medkd is totally unexpected and, as suggested by Organelli et al. (2017), “strongly warrants for further investigation”.

4 Conclusions

This work presented the latest achievements in the operational processing chain for ocean colour data stream for the Mediterranean Sea in the context of the European Copernicus Marine Environment Monitoring Service. The development of 30 the multi-sensor merged product builds on the previous version of this chain, which was focused on parallel processing of single sensors (SeaWiFS, MODIS and MERIS, Volpe et al., 2012). The introduction of an operational multi-sensor merged product aims to meet the operational oceanography intrinsic requirement of “One Question One Answer”. Three main steps

Deleted: There is a significant difference between the biases computed when the most recent observations are used (REP_{AV} and Multi_{AV}) and over the entire time series, likely due to the number of matchups (44 vs 708) and range of Chl values (-0.04-2 vs -0.007-9) associated with the bio-optical and trophic regimes (Figure 1).

Deleted: kd490

Deleted: 1

Deleted: and

Deleted: kd490

Deleted: 7

Deleted: Figure 10

Deleted: a

were implemented: band-shifting, inter-sensor bias correction, and the sensor merging. The band-shifting is implemented exactly as in Melin and Sclep (2015), while the implementation of the inter-sensor bias correction differs from the OC-CCI technique (CCLB, 2016) in the temporal and spatial aggregation scales. The sensor-merging shown in this work is based on the use of the climatology as input to the smoothing procedure as described in Volpe et al. (2018). The output of this 5 processing chain is the Rrs spectrum that constitutes the input to all algorithms used to derive the various geophysical products. The Rrs computed with the multi-sensor merged approach shows good agreement when compared with in situ observations of the basin-scale MedBiOp dataset as well as the two fixed location AAOT and BOUSSOLE time series. Moreover, this work presents an updated version of the empirical algorithms for Chl and Kd retrievals for the Mediterranean Sea based on the extended MedBiOp dataset. The comparison with the in situ observations yields good results when applied 10 to both the Rrs derived from the CCIV3 processor and those derived from the multi-sensor merged processing shown here. This suggests the opportunity to use the proposed multi-sensor processing chain in the REP context as well.

5 Acknowledgements

We wish to thank the anonymous reviewers for detailed and pertinent comments that helped to greatly improve the manuscript. Giuseppe Zibordi, as PI of the AERONET-OC site of Venise, is warmly thanked for the Level-2 surface reflectance data processing and site maintenance. The authors are also grateful to the BOUSSOLE project for maintaining and providing high-quality surface reflectance data used for the validation of the satellite observations. The International Argo Project (a pilot programme of the Global Ocean Observing System) and the national programmes that contribute to it (<http://www.argo.ucsd.edu>, <http://argo.jcommops.org>) are very much acknowledged. The NASA Ocean Biology Processing Group is strongly acknowledged for providing Level-2 data used as input to the processing chain. This work has been performed in the context of the Ocean Colour Thematic Assembly Centre of Copernicus Marine Environment and Monitoring Service (Grant number: 77-CMEMS-TAC-OC-N).

6 References

- Antoine, D., Guevel, P., Desté, J.-F., Bécu, G., Louis, F., Scott, A., and Bardey, P., 2008. The “BOUSSOLE” Buoy – A New Transparent- to-Swell Taut Mooring Dedicated to Marine Optics: Design, Tests, and Performance at Sea. *J. Atmos. Oceanic Technol.*, 25, 968–989.

Bailey, S.W., Werdell, P.J., 2006. A multi-sensor approach for the on-orbit validation of ocean color satellite data products. *Remote Sens Environ.*, 102, 12–23.

Barnes, B. B., Cannizzaro, J. P., English, D. C., & Hu, C. (2019). Validation of VIIRS and MODIS reflectance data in coastal and oceanic waters: An assessment of methods. *Remote Sensing of Environment*, 220, 110-123.

Berthon, J. F., G. Zibordi, Doyle, J.P., Grossi, S., van der Linde, D. Targa, C., 2002. Coastal Atmosphere and Sea Time Series (CoASTS), Part 2: Data Analysis. NASA Technical Memorandum. 2002-206892 Vol. 20. S. B. Hooker and E. R. Firestone. Greenbelt, Maryland, NASA Goddard Space Flight Center: 25.

- Bouali, M., and Ignatov, F., 2014. Adaptive Reduction of Striping for Improved Sea Surface Temperature Imagery from Suomi National Polar-Orbiting Partnership (S-NPP) Visible Infrared Imaging Radiometer Suite (VIIRS), *J. Atmos. Oceanic Technol.*, 31, 150-163.
- Bricaud, A., Bosc, E., & Antoine, D., 2002. Algal biomass and sea surface temperature in the Mediterranean Basin - Intercomparison of data from various satellite sensors, and implications for primary production estimates. *Remote Sensing of Environment*, 81(2-3), 163-178.
- Brown, A.C., Huot, Y., Werdele, P.J., Gentili, B., Claustre, H., 2008. The origin and global distribution of second order variability in satellite ocean color and its potential applications to algorithm development. *Remote Sensing of Environment*, 112, 4186-4203.
- 10 CCI, 2016a. *Ocean Colour Climate Change Initiative Product User Guide*, pp. 47. <http://www.esa-oceancolour-cci.org/>.
- CCI, 2016b. *Ocean colour data bias correction and merging*. Ocean colour-Climate Change Initiative, algorithm theoretical basis document, version 3.7. pp. 36. <http://www.esa-oceancolour-cci.org/>.
- CCI, 2017. *Ocean Colour Climate Change Initiative (Phase Two). Climate Assessment Report*. AO-1/6207/09/I-LG, pp. 125. (http://esa-oceancolour-cci.org/?q=webfm_send/702)
- 15 Colella, S., Falcini, F., Rinaldi, E., Sammartino, M., Santoleri, R., 2016. Mediterranean Ocean Colour Chlorophyll Trends. *PLoS ONE* 11(6): e0155756. <https://doi.org/10.1371/journal.pone.0155756>
- D'Alimonte, D. and Zibordi, G., 2003. Phytoplankton Determination in an Optically Complex Coastal Region Using a Multilayer Perceptron Neural Network, *IEEE Geosci. Remote S.*, 41, 2861–2868.
- D'Alimonte, D., Mélin, F., Zibordi, G., Berthon, J.-F., 2003. Use of the novelty detection technique to identify the range of applicability of the empirical ocean color algorithms. *IEEE Trans. Geosci. Remote Sens.*, 41, 2833-2843.
- D'Alimonte, D., Zibordi, G., Kajiyama, T., Cunha, J.C., 2010. Monte Carlo code for high spatial resolution ocean color simulations, *Applied Optics* 49, 4936-4950.
- Dierssen, H., 2010. Perspectives on empirical approaches for ocean color remote sensing of chlorophyll in a changing climate. *Proc. Natl. Acad. Sci.* 107, 17073-17078.
- 20 D'Ortenzio, F., Marullo, S., Ragni, M., D'Alcalà, M. R., & Santoleri, R., 2002. Validation of empirical SeaWiFS algorithms for chlorophyll-a retrieval in the Mediterranean Sea: A case study for oligotrophic seas. *Remote Sensing of Environment*, 82(1), 79-94. [https://doi.org/10.1016/S0034-4257\(02\)00026-3](https://doi.org/10.1016/S0034-4257(02)00026-3).
- Laws, E. A., Archie, J. W., 1981. Appropriate use of regression analysis in marine biology. *Marine Biology*, 65(1), 13-16.
- Lee, Z.P., Carder, K.L., Arnone, B.A., 2002. Deriving inherent optical properties from water color: A multi-band quasi-analytical algorithm for optically deep waters, *Applied Optics*, 41, 5755-5772.
- Le Traon, P-Y., Antoine, D., Bentamy, A., Bonekamp, H., Breivik, L.A., Chapron, B., Corlett, G., Dibarbour, G., DiGiacomo, P., Donlon, C., Faugère, Y., Font, J., Girard-Ardhuin, F., Gohin, F., Johannessen, J.A., Kamachi, M., Lagerloef, G., Lambin, J., Larnicol, G., Le Borgne, P., Leuliette, E., Lindstrom, E., Martin, M.J., Maturi, E., Miller, L., Mingsen, L., Morrow, R., Reul, N., Rio, M-H., Roquet, H., Santoleri, R., Wilkin, J., 2015. Use of satellite observations for operational oceanography: recent achievements and future prospects. *Journal of Operational Oceanography*, 8 (sup1), s12-s27.
- Loew, A., Bell, W., Brocca, L., Bulgin, C. E., Burdanowitz, J., Calbet, X., Verhoelst, T., 2017. Validation practices for satellite-based Earth observation data across communities. *Reviews of Geophysics*, 55(3), 779-817. <http://doi.org/10.1002/2017RG000562>
- Manzella, G. M. R., Hopkins, T. S., Minnett, P. J., & Nacini, E., 1990. Atlantic water in the Strait of Sicily. *Journal of Geophysical Research*, 95(C2), 1569–1575.
- 40 Maritorena, S., Siegel, D. A., 2005. Consistent merging of satellite ocean color data sets using a bio-optical model. *Remote Sensing of Environment*, 94, 429-440.
- Mélin, F., and Sclep, G., 2015. Band shifting for ocean color multi-spectral reflectance data. *Opt. Exp.*, 23, 2262-2279. DOI:10.1364/OE.23.002262.
- 45 Mélin, F., Vantrepotte, V., Clerici, M., D'Alimonte, D., Zibordi, G., Berthon, J. F., Canuti, E., 2011. Multi-sensor satellite time series of optical properties and chlorophyll-a concentration in the Adriatic Sea. *Progress in Oceanography*, 91(3), 229–244. <http://doi.org/10.1016/j.pocean.2010.12.001>
- Mikelsons, K., Wang, M., Jiang, L., Bouali, M., 2014. Destriping algorithm for improved satellite-derived ocean color product imagery, *Opt. Express* 22, 28058-28070.

Deleted:

Deleted: 1

Deleted: Mélin, F., Vantrepotte, V., Chuprin, A., Grant, M., Jackson, T., & Sathyendranath, S., 2017. Assessing the fitness-for-purpose of satellite multi-mission ocean color climate data records: A protocol applied to OC-CCI chlorophyll-a data. *Remote Sensing of Environment*, 203, 139–151. <http://doi.org/10.1016/j.rse.2017.03.039>

Mobley, C.D., Werdell, J., Franz, B., Ahmad, Z., & Bailey, S. (2016). Atmospheric Correction for Satellite Ocean Color Radiometry. Mobley, C.D., Werdell, J., Franz, B., Ahmad, Z., & Bailey, S. NASA/TM-2016-217551, GSFC-E-DAA-TN35509.

Moore, T. S., Dowell, M. D., Bradt, S., Ruiz Verdu, A., 2014. An optical water type framework for selecting and blending retrievals from bio-optical algorithms in lakes and coastal waters. *Remote Sensing of Environment*, 143, 97–111. <http://doi.org/10.1016/j.rse.2013.11.021>.

Morel, A. and Prieur, L. (1977). Analysis of variations in ocean color. *Limnol. Oceanogr.* 22: 709-722.

Mueller, J. L., and Austin, R. W., 1995. Ocean Optics Protocols for SeaWiFS Validation, Revision 1, S.B. Hooker, E.R. Firestone, and J.G. Acker Ed., NASA Technical Memorandum 104566, Vol. 25, SeaWiFS Technical Report Series.

Mueller, J. L., 2000. SeaWiFS algorithm for the diffuse attenuation coefficient, K(490), using water-leaving radiances at 490 and 555 nm. In S. B. Hooker, & E. R. Firestone (Eds.), *SeaWiFS postlaunch calibration and validation analyses: Part 3*. NASA Tech. Memo. 2000-206892, vol. 11 (pp. 24 – 27). Greenbelt' NASA Goddard Space Flight Center.

O'Reilly, J. E., Maritorena, S., Siegel, D., O'Brien, M. C., Toole, D., Mitchell, B. G., Culver, M., 2000. Ocean color chlorophyll a algorithms for SeaWiFS, OC2, and OC4: version 4. In S. B. Hooker & E. R. Firestone (Eds.), *SeaWiFS Postlaunch Technical Report Series*, vol.11. *SeaWiFS postlaunch calibration and validation analyses: part 3* (pp. 9–23). Greenbelt, MD: NASA Goddard Space Flight Center.

Organelli Emanuele, Barboux Marie, Clastre Hervé, Schmechtig Catherine, Poteau Antoine, Bricaud Annick, Uitz Julia, D'ortenzio Fabrizio, Dall'olmo Giorgio (2016). A global bio-optical database derived from Biogeochemical Argo float measurements within the layer of interest for field and remote ocean color applications. SEANOE. <https://doi.org/10.17882/47142>.

Organelli, E., Barboux, M., Clastre, H., Schmechtig, C., Poteau, A., Bricaud, A., Boss, E., Briggs, N., Dall'Olmo, G., D'Ortenzio, F., Leymarie, E., Mangin, A., Obolensky, G., Penkerc'h, C., Prieur, L., Roessler, C., Serra, R., Uitz, J., and Xing, X.: Two databases derived from BGC-Argo float measurements for marine biogeochemical and bio-optical applications, *Earth Syst. Sci. Data*, 9, 861–880, <https://doi.org/10.5194/essd-9-861-2017>, 2017.

Pitarch, J., Bellacicco, M., Volpe, G., Colella, S., & Santoleri, R. (2016). Use of the quasi-analytical algorithm to retrieve backscattering from in-situ data in the Mediterranean Sea. *Remote Sensing Letters*, 7(6), 591-600.

Santoleri, R., Volpe, G., Marullo, S., Buongiorno Nardelli, B., 2008. Open Waters Optical Remote Sensing of the Mediterranean Sea, in: *Remote Sensing of the European Seas*, edited by: Barale, V. and Gade, M., Springer, 103–116.

Sathyendranath, S., Brewin, R.J.W., Frédéric Mélin, T. J., Platt, T., 2017. Ocean-colour products for climate-change studies: What are their ideal characteristics?, *Remote Sensing of Environment*, <http://dx.doi.org/10.1016/j.rse.2017.04.017>

Steinmetz, F., Deschamps, P.-Y., Ramon, D., 2011. Atmospheric correction in the presence of sun glint: application to MERIS. *Opt. Express* 19, 9783–9800.

Szeto, M., Werdell, P. J., Moore, T. S., Campbell, J. W., 2011. Are the world's oceans optically different? *J. Geophys. Res.*, 116, C00H04, doi:10.1029/2011JC007230.

Teruzzi, A., Dobricic, S., Solidoro, C., Cossarini, G., 2014. A 3-D variational assimilation scheme in coupled transport-biogeochemical models: Forecast of Mediterranean biogeochemical properties, *J. Geophys. Res. Oceans*, 119, 200–217, doi:10.1002/2013JC009277.

Thuillier, G., Labs, D., Foujols, T., Peetermans, W., Gillotay, D., Simon, P. C., Mandel, H. 2003. The solar spectral irradiance from 200 to 2400 nm as measured by the SOLSPEC spectrometer from the ATLAS and EURECA missions, 1–22.

Valente, A., Sathyendranath, S., Brotas, V., Groom, S., Grant, M., Taberner, M., Antoine,D., Amone, R., Balch, W.M., Barker, K., Barlow, R., Bélanger, S., Berthon, J.F., Besiktepe, S., Brando, V., Canuti, E., Chavez, F., Clastre, H., Crout, R., Frouin, R., García-Soto, C., Gibb, S.W., Gould, R., Hooker, S., Kahru, M., Klein, H., Kratzer,S., Loisel, H., McKee, D., Mitchell, B.G., Moisan, T., Muller-Karger, F., O'Dowd, L., Ondrussek, M., Poulton, A.J., Repeta, M., Smyth, T., Sosik, H.M., Twardowski, M., Voss, K., Werdell, J., Wermand, M., Zibordi, G., 2016. A compilation of global bio-optical in situ data for ocean-colour satellite applications. *Earth Syst. Sci. Data* 8,235–252. <http://www.earth-syst-sci-data.net/8/235/2016/>. <http://dx.doi.org/10.5194/essd-8-235-2016>.

Volpe, G., Santoleri, R., Vellucci, V., Ribera d'Alcalà, M., Marullo, S., D'Ortenzio, F., 2007. The colour of the Mediterranean Sea: Global versus regional bio-optical algorithms evaluation and implication for satellite chlorophyll estimates, *Remote Sens. Environ.*, 107, 625–638.

Deleted: 1

Deleted: Pitarch, J., Volpe, G., Colella, S., Krasemann, H., and Santoleri, R., 2016. Remote sensing of chlorophyll in the Baltic Sea at basin scale from 1997 to 2012 using merged multi-sensor data, *Ocean Sci.*, 12, 379–389, <https://doi.org/10.5194/os-12-379-2016>.

- Volpe, G., Colella, S., Forneris, V., Tronconi, C., Santoleri, R., 2012. The Mediterranean Ocean Colour Observing System – system development and product validation. *Ocean Sci.*, 8, 869–883.
- Volpe, G., Buongiorno Nardelli, B., Colella, S., Pisano, A., Santoleri, R., 2018. An Operational Interpolated Ocean Colour Product in the Mediterranean Sea, in *New Frontiers in Operational Oceanography*, Ed. E.P. Chassignet, A. Pascual, J. Tintoré and J. Verron
- von Schuckmann, K., Le Traon, P.-Y., Alvarez-Fanjul, E., Axell, L., Balmaseda, M., Breivik, L.-A., Verbrugge, N., 2017. The Copernicus Marine Environment Monitoring Service Ocean State Report. *Journal of Operational Oceanography*, 9(sup2), s235–s320. <http://doi.org/10.1080/1755876X.2016.1273446>
- Zibordi, G., D'Alimonte, D., Berthon, J. F., 2004. An evaluation of depth resolution requirements for optical profiling in coastal waters. *Journal of Atmospheric and Oceanic Technology*, 21(7), 1059–1073. [https://doi.org/10.1175/1520-0426\(2004\)021<1059:AEODRR>2.0.CO;2](https://doi.org/10.1175/1520-0426(2004)021<1059:AEODRR>2.0.CO;2)
- Zibordi, G. and G. M. Ferrari, 1995. Instrument self-shading in underwater optical measurements: experimental data, *Appl. Opt.* 34, 2750-2754.
- Zibordi, G., Hooker, S.B., Berthon, J.-F., D'Alimonte, D., 2002. Autonomous above-water radiance measurements from an offshore platform: a field assessment experiment. *J. Atmos. Oceano. Tech.*, 19, 808-819.
- Zibordi, G., Mélin, F., Berthon, J.F., Holben, B., Slutsker, I., Giles, D., D'Alimonte, D., Vandemark, D., Feng, H., Schuster, G., Fabbri, B.E., 2009. AERONET-OC: a network for the validation of ocean color primary products. *Journal of Atmospheric and Oceanic Technology*, 26(8), pp.1634-1651.
- Zibordi, G., Berthon, J.-F., Mélin, F., D'Alimonte, D., 2011. Cross-site consistent in situ measurements for satellite ocean color applications: the BiOMap radiometric dataset. *Rem. Sens. Environ.*, 115, 2104–2115.
- Zibordi, G., Ruddick, K., Ansko, I., Moore, G., Kratzer, S., Icely, J., & Reinart, A. (2012). In situ determination of the remote sensing reflectance: An inter-comparison. *Ocean Science*, 8(4), 567–586. <https://doi.org/10.5194/os-8-567-2012>.

Deleted: , in press

7 Figures

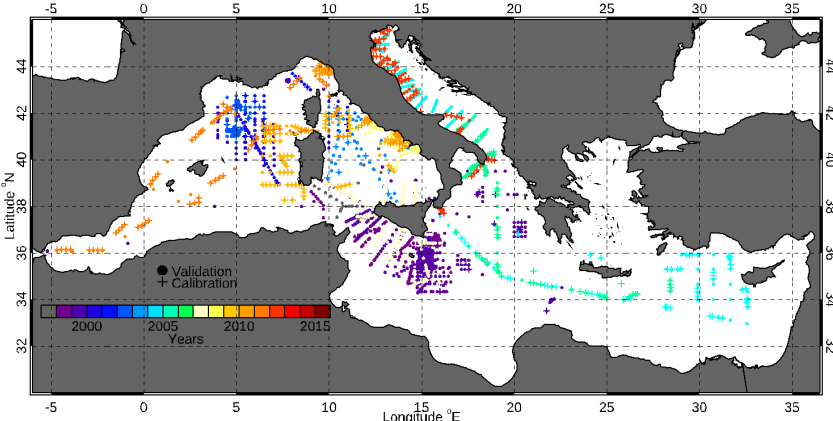


Figure 1: Study Area and space-time distribution of the in situ MedBiOp dataset (1997–2016) used in this work. Dots identify the in situ station used as sea-truth for satellite data validation, whereas crosses refer to the observations used to develop the regional OC algorithms.

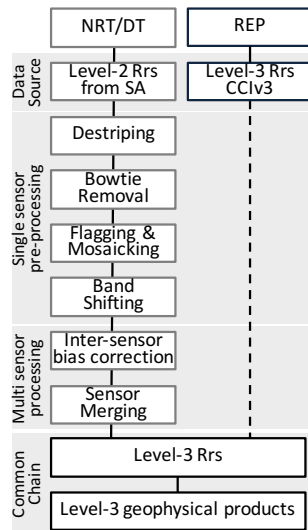


Figure 2: flowchart of the processing chains for the two data production lines, NRT/DT and REP modes. SA stands for space agencies. The dashed vertical line indicates that, the CNR REP processing mode only involves the application of the regional fine-tuned algorithms for the retrieval of the geophysical quantities.

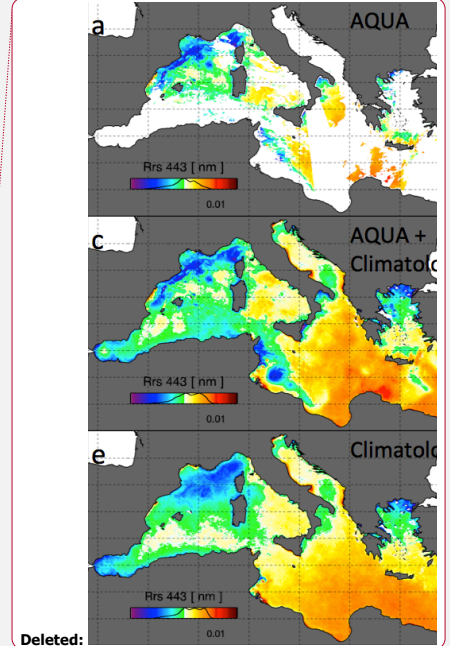
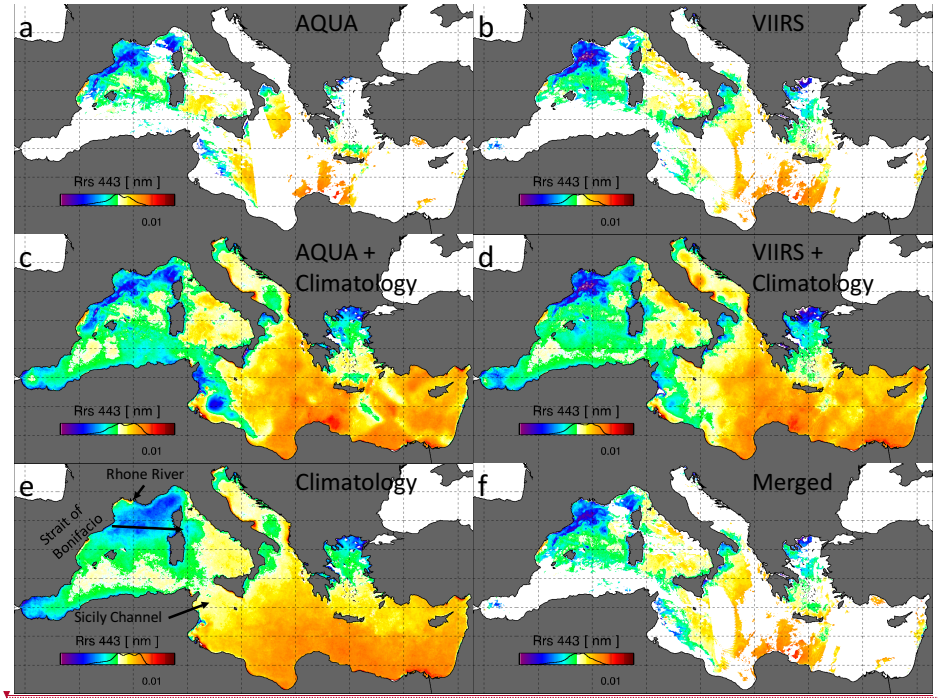


Figure 3: Example of how the merging of MODIS and VIIRS works. Rrs 443 from MODIS AQUA (a), NPP-VIIRS (b) from April 1st 2012. Panels c and d are obtained by filling in panels a and b with daily climatology (e). The merged multi sensor product is obtained after removal of the unseen pixels (f).

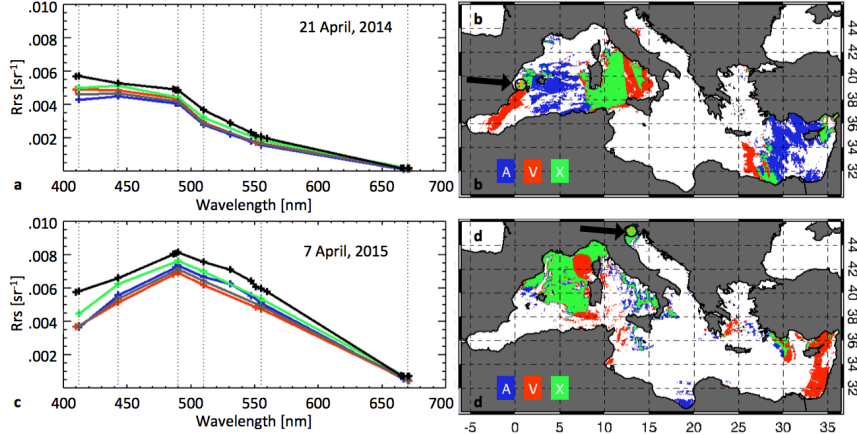


Figure 4: Rrs spectra from the 21st April, 2014 (panel a), from MODIS-AQUA (A, blue), NPP-VIIRS (V, red), the merged multi-sensor product with the application of the bias correction (X, green) and without (grey), and the in situ measurements (black), all in correspondence of the in situ measurement location shown by the arrow in panel b. The map in panel b is the sensor mask of the day in which the pixels sampled by MODIS-AQUA only are shown in blue and those by NPP-VIIRS only in red; the pixels sampled by both sensors are shown in green. Panel c and d refer to the Rrs spectra and sensor mask from the 7th April 2015, in the northern Adriatic Sea.

5

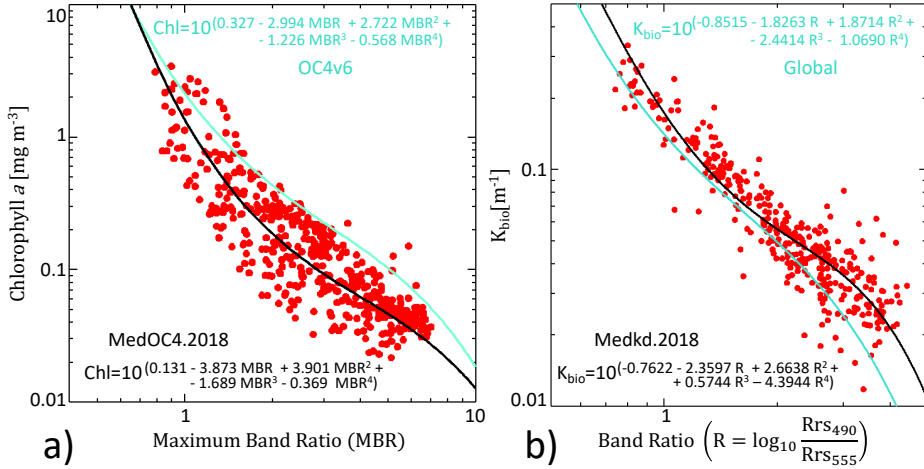
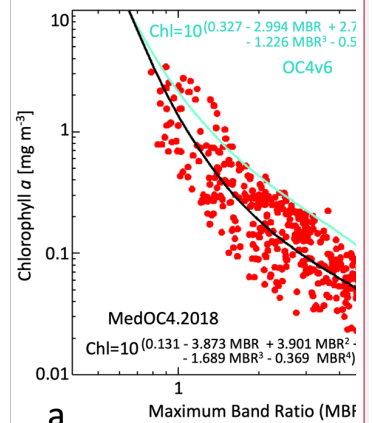


Figure 5: panel a: algorithm for chlorophyll retrieval over the Mediterranean Sea. The maximum band ratio (MBR) is shown on the X-axis; it is the \log_{10} ratio between the maximum value between the three bands in the blue (443, 490 and 510 nm) and the one in the green part of the light spectrum (555 nm). Red dots ($N=509$) are the in situ bio-optical data (whose location is shown in Figure 1) used to compute the operational algorithm (black line). As a means of comparison the global algorithm (OC4v6, https://oceancolor.gsfc.nasa.gov/atbd/chlor_a) functional form is also superimposed (turquoise line). Panel b: algorithm for the retrieval of the diffuse attenuation coefficient, K_{d490} , over both the Mediterranean Sea (black line) and the global ocean (turquoise line). The global algorithm is the SeaWiFS (https://oceancolor.gsfc.nasa.gov/atbd/kd_490). Red dots ($N=366$) are the in situ measurements over the Mediterranean Sea. K_{d490} is the sum of K_{bio} and of the attenuation due to pure sea water (0.0166; [Mueller, 2000](#)).



Deleted:

Deleted: K_{d490}

Deleted: Differently than for Chl, here on the X-axis, the ratio between $R_{\text{rs}490}$ and $R_{\text{rs}555}$ is shown.

Deleted: K_{d490}

Deleted: Pope and Fry, 197

Deleted: 2

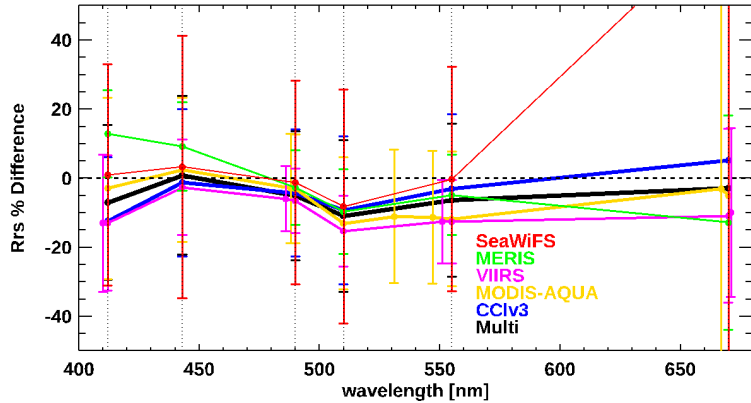
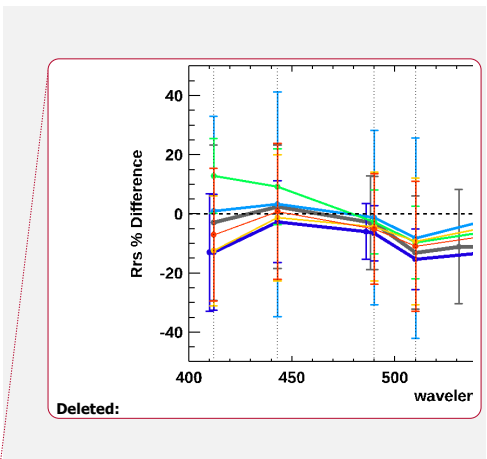


Figure 6: Relative difference between satellite and MedBiOp Rrs spectra for MODIS-Aqua (yellow), NPP-VIIRS (magenta), SeaWiFS (red), MERIS (green), OC-CCI (blue) and for the multi-sensor product developed and described in this work (black). Vertical bars represent one standard deviation from the average RPD value. Target wavelengths are marked with vertical dotted lines.

5



- Deleted: grey
- Deleted: blue
- Deleted: turquoise
- Deleted: yellow
- Deleted: red

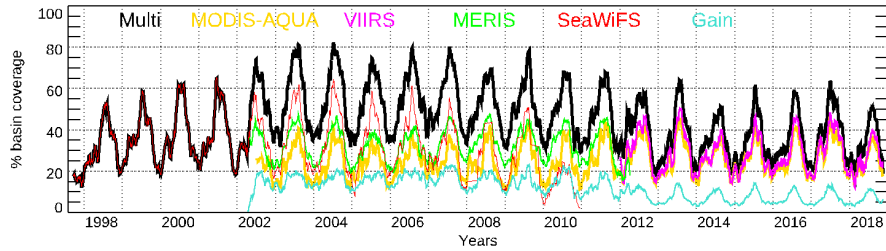


Figure 7: Time series of the number of pixels for each satellite sensor as percent with respect to the basin total coverage. For the sake of readability, each line represents the result of the 30 days running median time series. Turquoise line is the basin coverage increase that is gained with the Multi with respect to the maximum coverage from the single sensors.

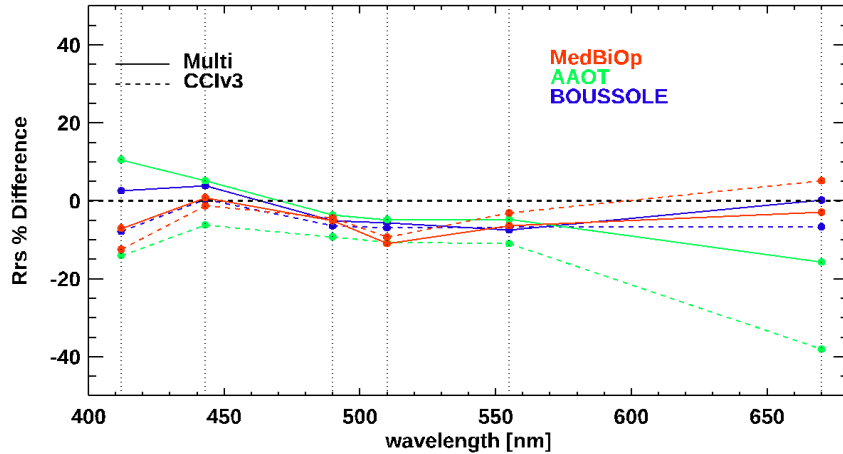


Figure 8: Relative difference between Multi and CCIv3 satellite observations and in situ measurements (MedBiOp in red, AAOT in green and BOUSSOLE in blue). The number of matchups used from each dataset is summarized in Table 3. Target wavelengths are marked with vertical dotted lines. As a reference the two red lines correspond to the red and orange lines in Figure 6.

Deleted: Table 3

Deleted: Figure 6

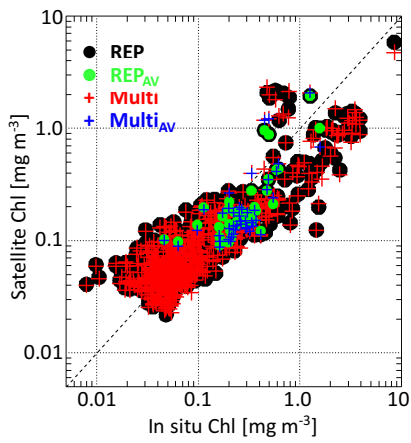
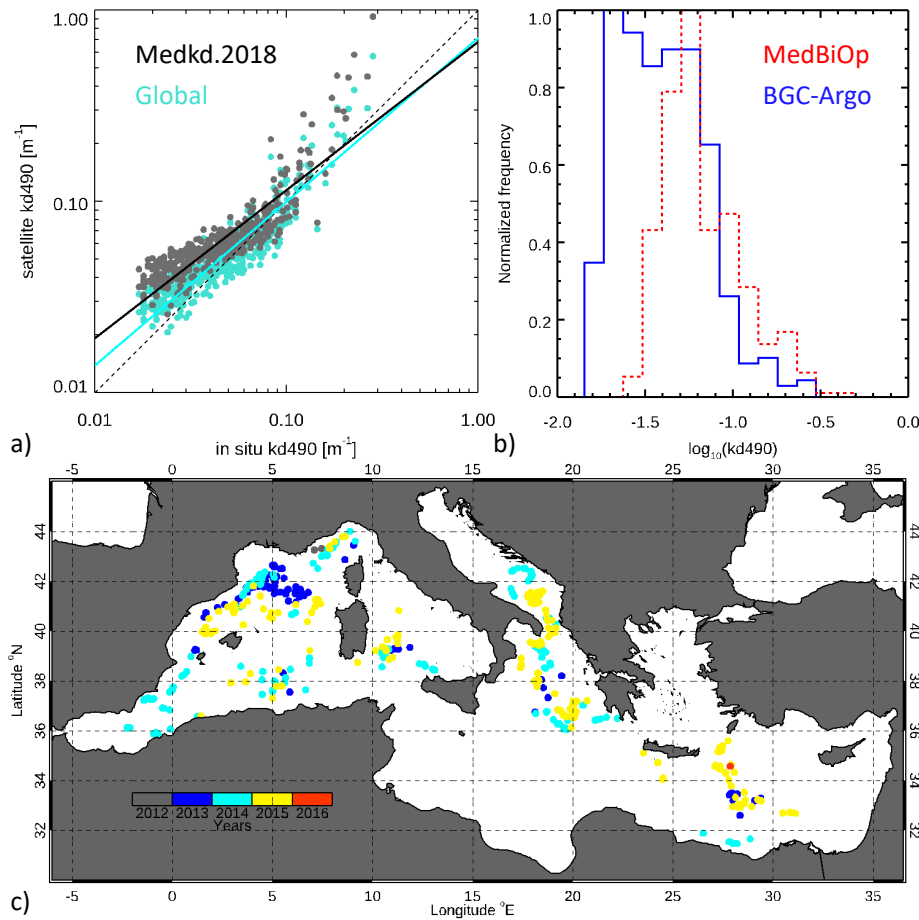


Figure 9: Satellite (y axis) versus in situ (MedBiOp) Chl concentration. Satellite Chl is the REP (derived by the application of the MedOC4.2018 to the Rrs derived from the CCIv3 processor, black) and NRT (derived from the Multi processing, red). Green dots

Deleted: 7

and blue crosses are the REP and NRT for matchups on the period in which VIIRS and MODIS co-exist (REP_{AV} and Multi_{AV}). Statistics associated with the matchup comparison are shown in [Table 4](#).

Deleted: Table 4



5 **Figure 10:** Satellite kd validation with the BGC-Argo float dataset (Organelli et al., 2016). Panel a shows the in situ kd (x axis) versus the satellite-derived kd obtained with the Medkd.2018 (grey dots) and the Global algorithm (turquoise dots), respectively, as shown in Figure 5b. The two best-fit lines are also superimposed. The normalized frequency distribution of the two in situ

Deleted: 7

Deleted: black

kd490 measurements (MedBiOp in red and the BGC-Argo in blue) is shown in Panel b. The space-time distribution of the matchups is shown in panel b. Relevant statistics are available in Supplementary Material (Table S.9).

8 Tables

5

Wavelength (nm)	Sensors					
	VIIRS	MODIS	MERIS	OLCI	SeaWiFS	REP
410	•					
412		•			•	•
413			•	•		
443	•	•	•	•	•	•
486	•					
488		•				
490			•	•	•	•
510			•	•	•	•
531	•					
547		•				
551	•					
555					•	•
560			•	•		
665			•	•		•
667		•				
670					•	•
671	•					

Table 1: Overview of the available wavelengths from VIIRS, MODIS, MERIS, OLCI and SeaWiFS sensors and those used to produce the REP dataset (available from PML) and those collected in situ. Target wavelengths of the band shifting procedure are highlighted in grey. Column “in situ” refers to the bands of the Lu, Ed and Es Satlantic radiometers used to compute the algorithm functional forms and described in the in situ data description section ([The Mediterranean Sea in situ bio-optical dataset: MedBiOp](#)).

10

Deleted: The Mediterranean Sea in situ bio-optical dataset: MedBiOp

Name	Definition
------	------------

Type-2 slope	$S = \frac{\sum_{i=1}^N (X_i^E - \bar{X}^E)^2 - \sum_{i=1}^N (X_i^M - \bar{X}^M)^2 + \left[\sum_{i=1}^N (X_i^E - \bar{X}^E)^2 - \sum_{i=1}^N (X_i^M - \bar{X}^M)^2 \right] + 4 \sum_{i=k}^N (X_k^E - \bar{X}^E)(X_k^M - \bar{X}^M)}{2 \sum_{i=k}^N (X_k^E - \bar{X}^E)(X_k^M - \bar{X}^M)}$
Type-2 intercept	$I = \bar{X}^E - S \cdot \bar{X}^M$
Determination coefficient	$r^2 = \frac{\left[\sum_{i=1}^N (X_i^E - \bar{X}_i^E)(X_i^M - \bar{X}_i^M) \right]^2}{\sum_{i=1}^N (X_i^E - \bar{X}_i^E)^2 \sum_{i=1}^N (X_i^M - \bar{X}_i^M)^2}$
Root Mean Square Difference	RMSD = $\sqrt{\frac{\sum_{i=1}^N (X_i^E - X_i^M)^2}{N}}$
Bias	bias = $\frac{1}{N} \sum_{i=1}^N (X_i^E - X_i^M)$
Relative percentage Difference	RPD = $100 \cdot \frac{1}{N} \sum_{i=1}^N \frac{ X_i^E - X_i^M }{X_i^M}$
Absolute percentage Difference	APD = $100 \cdot \frac{1}{N} \sum_{i=1}^N \frac{ X_i^E - X_i^M }{X_i^M}$

Table 2: Metrics used to compare the estimated (satellite-based) dataset X^E to a reference, measured in-situ dataset X^M . A more comprehensive table of metrics is provided in Supplementary Material (Table S.1).

Rrs	Slope	Intercept	r^2	RMSD	Bias	RPD	APD	N
412	0.99	-0.0006	0.77	0.0015	-0.00060	-7	18	272
443	0.86	0.0007	0.73	0.0013	-0.00023	1	15	272
490	0.65	0.0015	0.55	0.0013	-0.00047	-5	13	272
510	0.65	0.0009	0.57	0.0013	-0.00060	-11	18	272
555	0.68	0.0005	0.71	0.0012	-0.00027	-6	16	272
670	1.19	-0.0001	0.91	0.0002	-0.00002	-3	35	197

Table 3: Statistics associated with the Multi Rrs product computed over the MedBiOp dataset. The same statistics associated with all products shown in Figure 6 are provided in Supplementary Material (Table S.2 to Table S.7).

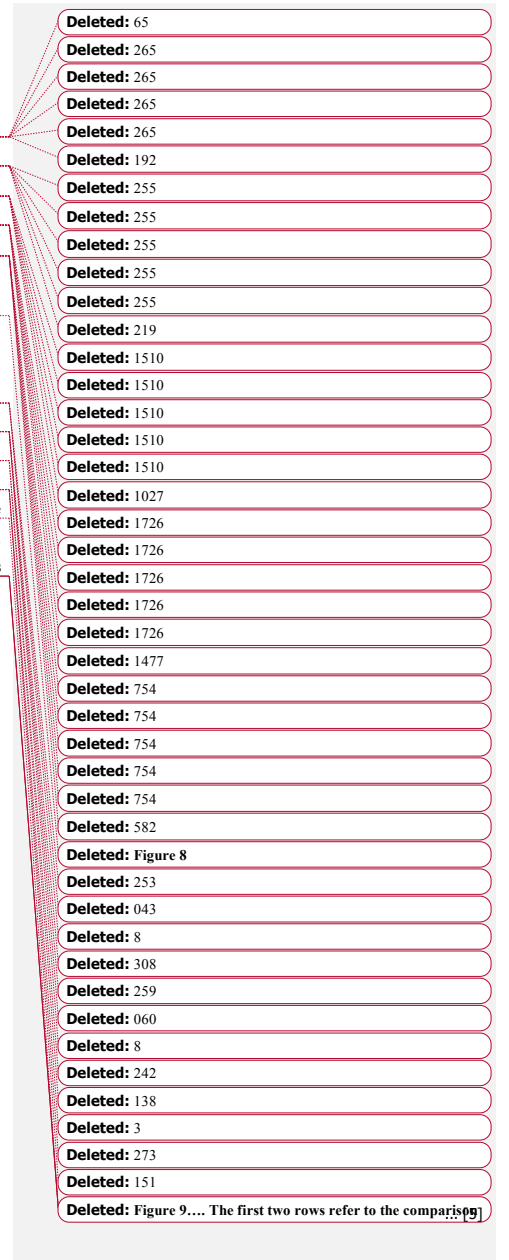
- Deleted: 78
- Deleted: 7
- Deleted: 85
- Deleted: 00022
- Deleted: 66
- Deleted: 00059
- Deleted: 00001
- Deleted: 1
- Deleted: 4
- Deleted: Figure 6
- Deleted: 4

		Bands [nm]					
in situ	Satellite	412	443	490	510	555	670
MedBiOp	Multi	272	272	272	272	272	197
	CCIV3	262	262	262	262	262	223
AAOT	Multi	1794	1794	1794	1794	1794	1301
	CCIV3	1753	1753	1753	1753	1753	1504
BOUSSOLE	Multi	961	961	961	961	961	780
	CCIV3	882	882	882	882	882	780

Table 4: Number of matchups used to compute the statistics presented in [Figure 8](#).

Product	Slope	Intercept	r ²	RMSD	Bias	RPD	APD	N
<i>REP</i>	0.737	-0.306	0.75	0.411	-0.093	7	47	710
<i>Multi</i>	0.752	-0.309	0.74	0.427	-0.098	3	47	710
<i>REP_{AV}</i>	1.052	-0.108	0.57	0.207	-0.064	-18	43	44
<i>Multi_{AV}</i>	1.184	-0.047	0.50	0.271	-0.057	-17	48	44

Table 5: Statistics about the three Chl matchup datasets described in [Figure 9](#). The first two rows refer to the comparison of the two satellite multi-sensor products with the entire MedBiOp Chl dataset, while the last two refer to the statistics associated with 5 matchups on the period in which VIIRS and MODIS co-exist (*REP_{AV}* and *Multi_{AV}*). A more comprehensive table of metrics is provided in Supplementary Material (Table S.8).



Page 6: [1] Deleted	Gianluca Volpe	11/26/18 12:34:00 PM
▼		
Page 9: [2] Deleted	Gianluca Volpe	10/23/18 2:17:00 PM
▼		
Page 9: [3] Deleted	Gianluca Volpe	10/23/18 2:30:00 PM
▼		
Page 9: [4] Deleted	Gianluca Volpe	10/23/18 3:08:00 PM
▼		
Page 30: [5] Deleted	Gianluca Volpe	11/28/18 2:54:00 PM
▼		
Page 30: [5] Deleted	Gianluca Volpe	11/28/18 2:54:00 PM
▼		
Page 30: [5] Deleted	Gianluca Volpe	11/28/18 2:54:00 PM
▼		

The Mediterranean Ocean Colour Level 3 Operational Multi-Sensor Processing

Gianluca Volpe¹, Simone Colella¹, Vittorio Brando¹, Vega Forneris¹, Flavio La Padula¹, Annalisa Di Cicco¹, Michela Sammartino¹, Marco Bracaglia^{1,2}, Florinda Artuso³, Rosalia Santoleri¹

¹Istituto di Scienze Marine, Via Fosso del Cavaliere 100, 00133, Roma, Italy

²Università degli Studi di Napoli Parthenope, Via Amm. F. Acton 38, 80133, Naples, Italy

³Agenzia nazionale per le nuove tecnologie, l'energia e lo sviluppo economico sostenibile, Dipartimento Ambiente, Centro Ricerche Frascati, Frascati, Italy

Correspondence to: Gianluca Volpe (gianluca.volpe@cnr.it)

Deleted: dell'Atmosfera e del Clima

Deleted: Ente

Deleted: per le Nuove tecnologie l'Energia e l'Ambiente

Supplementary Material

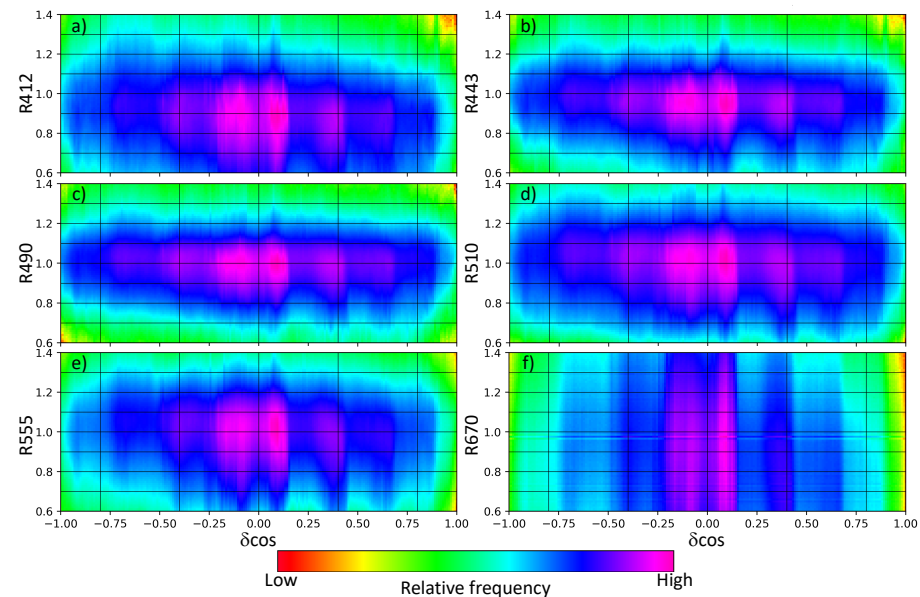


Figure S.1: 2D frequency histogram of the daily Rrs ratio (R , on the Y-axis) and of the difference of the cosine of the scattering angle ($\delta \cos$) between MODIS-AQUA and VIIRS for each of the six bands of the Multi product (2012-2017). The scattering angle (Θ_s) is defined as $\Theta_s = \frac{180}{\pi} \arccos \left(-\cos \left(\frac{\pi}{180} \theta_0 \right) \cos \left(\frac{\pi}{180} \theta_s \right) - \sin \left(\frac{\pi}{180} \theta_0 \right) \cos \left(\frac{\pi}{180} \varphi_r \right) \right)$, with $\theta_0, \theta_s, \varphi_r$ being the solar and sensor zenith angles and the relative azimuth angle, respectively. R exhibits a substantial variability across the spectrum with the values shown in panels a) and f) presenting the larger differences. Overall, the median values of the Rrs ratios at the six bands are within the range 0.9-1.1. The noticeable feature is the lack of any dependency of R from the geometry of the observation ($\delta \cos$).

Deleted: 1

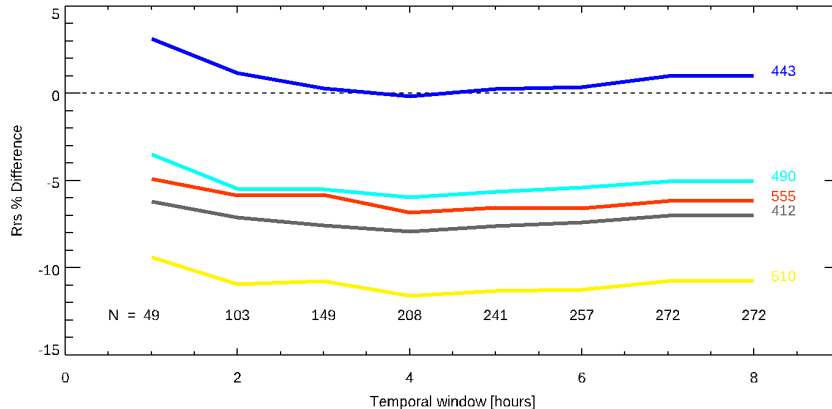


Figure S.2: Relative percent difference between Multi and in situ (MedBiOp) Rrs as function of the temporal window used for determining coincidence. Since the satellite pixel overpass time is lost because of the merging procedure, we assume here to be 12 am local time. Superimposed is also the number of matchups. The plot shows that after 3 hours the range of variability is always within 1%, while the number of points used and thus the significance increases.

Name	Definition
In situ data average	$\bar{X}^M = \frac{1}{N} \sum_{i=1}^N X_i^M$
Satellite data average	$\bar{X}^E = \frac{1}{N} \sum_{i=1}^N X_i^E$
Type-2 slope	$S = \frac{\sum_{i=1}^N (X_i^E - \bar{X}^E)^2 - \sum_{i=1}^N (X_i^M - \bar{X}^M)^2 + \left[\left\{ \sum_{i=1}^N (X_i^E - \bar{X}^E)^2 - \sum_{i=1}^N (X_i^M - \bar{X}^M)^2 \right\} + 4 \sum_{i=k}^N (X_k^E - \bar{X}^E)(X_k^M - \bar{X}^M) \right]^2}{2 \sum_{i=k}^N (X_k^E - \bar{X}^E)(X_k^M - \bar{X}^M)}$
Type-2 intercept	$I = \bar{X}^E - S \cdot \bar{X}^M$
Determination coefficient	$r^2 = \frac{\left[\sum_{i=1}^N (X_i^E - \bar{X}^E)(X_i^M - \bar{X}^M) \right]^2}{\sum_{i=1}^N (X_i^E - \bar{X}^E)^2 \sum_{i=1}^N (X_i^M - \bar{X}^M)^2}$

Root Mean Square Difference	$RMSD = \sqrt{\frac{\sum_{i=1}^N (X_i^E - X_i^M)^2}{N}}$
Centre-pattern Root Mean Square Difference	$cRMSD = \sqrt{\frac{\left[\sum_{i=1}^N \{ [X_i^E - (\sum_{j=1}^N X_j^E)] - [X_i^M - (\sum_{k=1}^N X_k^M)] \} \right]^2}{N}}$
Bias	$bias = \frac{1}{N} \sum_{i=1}^N (X_i^E - X_i^M)$
Mean Absolute Error	$MAE = \frac{1}{N} \sum_{i=1}^N X_i^E - X_i^M $
Relative percentage difference	$RPD = 100 \cdot \frac{1}{N} \sum_{i=1}^N \frac{ X_i^E - X_i^M }{X_i^M}$
Absolute percentage difference	$APD = 100 \cdot \frac{1}{N} \sum_{i=1}^N \frac{ X_i^E - X_i^M }{X_i^M}$

Table S.1: Metrics used to compare the estimated (satellite-based) dataset XE to a reference, measured in-situ dataset XM. The centre-pattern (or unbiased) Root Mean Square Distance (cRMSD) describes the error of the estimated values with respect to the measured ones, regardless of the average bias between the two distributions.

Deleted: RRS

... [1]

<u>RRS</u>	<u>\bar{X}^M</u>	<u>\bar{X}^E</u>	<u>Slope</u>	<u>Intercept</u>	<u>r^2</u>	<u>RMSD</u>	<u>cRMSD</u>	<u>Bias</u>	<u>MAE</u>	<u>RPD</u>	<u>APD</u>	<u>N</u>
<u>412</u>	<u>0.0059</u>	<u>0.0056</u>	<u>1.01</u>	<u>-0.0004</u>	<u>0.75</u>	<u>0.0013</u>	<u>0.0013</u>	<u>-0.00030</u>	<u>0.00098</u>	<u>-3</u>	<u>19</u>	<u>155</u>
<u>443</u>	<u>0.0056</u>	<u>0.0056</u>	<u>0.94</u>	<u>0.0003</u>	<u>0.80</u>	<u>0.0010</u>	<u>0.0010</u>	<u>-0.00004</u>	<u>0.00072</u>	<u>2</u>	<u>15</u>	<u>155</u>
<u>488</u>	<u>0.0052</u>	<u>0.0050</u>	<u>0.96</u>	<u>0.0000</u>	<u>0.79</u>	<u>0.0007</u>	<u>0.0007</u>	<u>-0.00025</u>	<u>0.00056</u>	<u>-3</u>	<u>12</u>	<u>155</u>
<u>490</u>	<u>0.0052</u>	<u>0.0050</u>	<u>0.96</u>	<u>0.0000</u>	<u>0.79</u>	<u>0.0007</u>	<u>0.0007</u>	<u>-0.00025</u>	<u>0.00056</u>	<u>-3</u>	<u>12</u>	<u>155</u>
<u>510</u>	<u>0.0040</u>	<u>0.0035</u>	<u>1.08</u>	<u>-0.0009</u>	<u>0.79</u>	<u>0.0008</u>	<u>0.0006</u>	<u>-0.00057</u>	<u>0.00072</u>	<u>-13</u>	<u>19</u>	<u>155</u>
<u>531</u>	<u>0.0033</u>	<u>0.0029</u>	<u>1.05</u>	<u>-0.0005</u>	<u>0.88</u>	<u>0.0006</u>	<u>0.0005</u>	<u>-0.00037</u>	<u>0.00053</u>	<u>-11</u>	<u>18</u>	<u>155</u>
<u>547</u>	<u>0.0027</u>	<u>0.0024</u>	<u>1.02</u>	<u>-0.0004</u>	<u>0.91</u>	<u>0.0005</u>	<u>0.0004</u>	<u>-0.00030</u>	<u>0.00044</u>	<u>-11</u>	<u>18</u>	<u>155</u>
<u>555</u>	<u>0.0025</u>	<u>0.0022</u>	<u>1.03</u>	<u>-0.0004</u>	<u>0.92</u>	<u>0.0005</u>	<u>0.0004</u>	<u>-0.00028</u>	<u>0.00041</u>	<u>-12</u>	<u>18</u>	<u>155</u>
<u>667</u>	<u>0.0003</u>	<u>0.0003</u>	<u>1.57</u>	<u>-0.0002</u>	<u>0.88</u>	<u>0.0002</u>	<u>0.0002</u>	<u>-0.00001</u>	<u>0.00010</u>	<u>-3</u>	<u>35</u>	<u>117</u>
<u>670</u>	<u>0.0003</u>	<u>0.0003</u>	<u>1.54</u>	<u>-0.0002</u>	<u>0.89</u>	<u>0.0002</u>	<u>0.0002</u>	<u>-0.00001</u>	<u>0.00009</u>	<u>-5</u>	<u>34</u>	<u>127</u>

Table S.2: Statistics associated with the MODIS-AQUA Rrs computed over the MedBiOp dataset.

<u>RRS</u>	<u>\bar{X}^M</u>	<u>\bar{X}^E</u>	<u>Slope</u>	<u>Intercept</u>	<u>r2</u>	<u>RMSD</u>	<u>cRMSD</u>	<u>Bias</u>	<u>MAE</u>	<u>RPD</u>	<u>APD</u>	<u>N</u>
<u>410</u>	<u>0.0049</u>	<u>0.0043</u>	<u>1.41</u>	<u>-0.0026</u>	<u>0.44</u>	<u>0.0011</u>	<u>0.0009</u>	<u>-0.00065</u>	<u>0.00092</u>	<u>-13</u>	<u>19</u>	<u>93</u>
<u>412</u>	<u>0.0049</u>	<u>0.0043</u>	<u>1.39</u>	<u>-0.0026</u>	<u>0.45</u>	<u>0.0011</u>	<u>0.0009</u>	<u>-0.00065</u>	<u>0.00092</u>	<u>-13</u>	<u>19</u>	<u>93</u>
<u>443</u>	<u>0.0049</u>	<u>0.0048</u>	<u>0.97</u>	<u>0.0000</u>	<u>0.63</u>	<u>0.0007</u>	<u>0.0007</u>	<u>-0.00018</u>	<u>0.00054</u>	<u>-3</u>	<u>11</u>	<u>93</u>
<u>486</u>	<u>0.0052</u>	<u>0.0049</u>	<u>0.92</u>	<u>0.0001</u>	<u>0.86</u>	<u>0.0006</u>	<u>0.0005</u>	<u>-0.00034</u>	<u>0.00049</u>	<u>-6</u>	<u>9</u>	<u>93</u>
<u>490</u>	<u>0.0052</u>	<u>0.0049</u>	<u>0.93</u>	<u>0.0000</u>	<u>0.87</u>	<u>0.0006</u>	<u>0.0005</u>	<u>-0.00037</u>	<u>0.00050</u>	<u>-6</u>	<u>9</u>	<u>93</u>
<u>510</u>	<u>0.0044</u>	<u>0.0037</u>	<u>1.02</u>	<u>-0.0007</u>	<u>0.92</u>	<u>0.0008</u>	<u>0.0005</u>	<u>-0.00065</u>	<u>0.00069</u>	<u>-15</u>	<u>16</u>	<u>93</u>
<u>551</u>	<u>0.0031</u>	<u>0.0027</u>	<u>0.99</u>	<u>-0.0003</u>	<u>0.95</u>	<u>0.0006</u>	<u>0.0005</u>	<u>-0.00036</u>	<u>0.00045</u>	<u>-12</u>	<u>15</u>	<u>93</u>
<u>555</u>	<u>0.0030</u>	<u>0.0027</u>	<u>1.00</u>	<u>-0.0003</u>	<u>0.95</u>	<u>0.0006</u>	<u>0.0005</u>	<u>-0.00035</u>	<u>0.00044</u>	<u>-13</u>	<u>15</u>	<u>93</u>
<u>670</u>	<u>0.0005</u>	<u>0.0005</u>	<u>1.14</u>	<u>-0.0001</u>	<u>0.95</u>	<u>0.0002</u>	<u>0.0002</u>	<u>-0.00003</u>	<u>0.00010</u>	<u>-11</u>	<u>20</u>	<u>50</u>
<u>671</u>	<u>0.0005</u>	<u>0.0005</u>	<u>1.14</u>	<u>-0.0001</u>	<u>0.95</u>	<u>0.0002</u>	<u>0.0002</u>	<u>-0.00003</u>	<u>0.00010</u>	<u>-10</u>	<u>20</u>	<u>49</u>

Table S.3: Statistics associated with the VIIRS Rrs computed over the MedBiOp dataset.

Deleted: 
 RRS

... [3]

Deleted: RRS

... [4]

RRS	\bar{X}^M	\bar{X}^E	SLOPE	INTERCEPT	R ²	RMSD	CRMSE	BIAS	MAE	RPD	APD	N
412	0.0085	0.0082	1.04	-0.0007	0.64	0.0019	0.0018	-0.00031	0.00146	1	21	98
443	0.0078	0.0076	0.92	0.0003	0.62	0.0016	0.0016	-0.00028	0.00120	3	21	98
490	0.0059	0.0056	0.69	0.0015	0.32	0.0013	0.0013	-0.00036	0.00092	-1	17	98
510	0.0040	0.0034	0.15	0.0029	0.02	0.0012	0.0011	-0.00053	0.00084	-8	22	98
555	0.0019	0.0018	0.26	0.0013	0.03	0.0007	0.0007	-0.00009	0.00039	0	20	98
670	0.0002	0.0003	11.16	-0.0017	0.08	0.0002	0.0001	0.00011	0.00012	76	80	40

Table S.4: Statistics associated with the SeaWiFS Rrs computed over the MedBiOp dataset.

<u>RRS</u>	<u>\bar{X}^M</u>	<u>\bar{X}^E</u>	<u>SLOPE</u>	<u>INTERCEPT</u>	<u>R²</u>	<u>RMSD</u>	<u>CRMSE</u>	<u>BIAS</u>	<u>MAE</u>	<u>RPD</u>	<u>APD</u>	<u>N</u>	<u>\bar{X}^M</u>	
<u>412</u>	Mrrs412	0.0083	0.0092		0.97	0.0011	0.90	0.0012	0.0009	0.00089	0.00104	13	14	90
<u>443</u>	Mrrs443	0.0076	0.0081		0.85	0.0016	0.86	0.0010	0.0009	0.00046	0.00072	9	12	90
<u>490</u>	Mrrs490	0.0060	0.0057		0.56	0.0023	0.79	0.0011	0.0010	-0.00031	0.00056	-3	8	90
<u>510</u>	Mrrs510	0.0042	0.0036		0.54	0.0014	0.87	0.0011	0.0010	-0.00051	0.00061	-10	13	90
<u>560</u>	Mrrs555	0.0022	0.0019		0.54	0.0008	0.95	0.0012	0.0012	-0.00022	0.00030	-5	10	90
<u>670</u>	Mrrs670	0.0002	0.0002		1.17	-0.0001	0.74	0.0001	0.0001	-0.00003	0.00005	-13	28	72

Table S.5: Statistics associated with the MERIS Rrs computed over the MedBiOp dataset.

Deleted:  RRS

... [5]

Deleted: RRS

... [6]

RRS	\bar{X}^M	\bar{X}^E	SLOPE	INTERCEPT	R ²	RMSD	CRMSE	BIAS	MAE	RPD	APD	N
412	0.0069	0.0060	0.97	-0.0007	0.83	0.0015	0.0012	-0.00087	0.00112	-12	17	262
443	0.0066	0.0063	0.86	0.0006	0.82	0.0011	0.0011	-0.00030	0.00077	-1	13	262
490	0.0057	0.0053	0.75	0.0010	0.72	0.0010	0.0009	-0.00040	0.00067	-4	12	262
510	0.0042	0.0037	0.80	0.0003	0.74	0.0010	0.0009	-0.00051	0.00067	-9	16	262
555	0.0025	0.0023	0.80	0.0003	0.84	0.0008	0.0008	-0.00017	0.00038	-3	14	262
670	0.0003	0.0003	0.97	0.0000	0.87	0.0001	0.0001	-0.00001	0.00009	5	38	223

Table S.6: Statistics associated with CCIv3 Rrs computed over the MedBiOp dataset.

RRS	\bar{X}^M	\bar{X}^E	SLOPE	INTERCEPT	R²	RMSD	CRMSE	BIAS	MAE	RPD	APD	N
412	0.0070	0.0064	0.99	-0.0006	0.77	0.0015	0.0014	-0.00060	0.00113	-7	18	272
443	0.0066	0.0064	0.86	0.0007	0.73	0.0013	0.0013	-0.00023	0.00089	1	15	272
490	0.0057	0.0052	0.65	0.0015	0.55	0.0013	0.0012	-0.00047	0.00077	-5	13	272
510	0.0042	0.0037	0.65	0.0009	0.57	0.0013	0.0011	-0.00060	0.00077	-11	18	272
555	0.0025	0.0022	0.68	0.0005	0.71	0.0012	0.0012	-0.00027	0.00044	-6	16	272
670	0.0003	0.0003	1.19	-0.0001	0.91	0.0002	0.0002	-0.00002	0.00008	-3	35	197

Table S.7: Statistics associated with the Multi Rrs computed over the MedBiOp dataset.

Deleted:  RRS

... [7]

CHL	\bar{X}^M	\bar{X}^E	SLOPE	INTERCEPT	r^2	RMSD	CRMSE	BIAS	MAE	RPD	APD	N
REP	0.257	0.163	0.737	-0.306	0.75	0.411	0.400	-0.093	0.143	7	47	710
MULTI	0.257	0.158	0.752	-0.309	0.74	0.427	0.415	-0.098	0.146	3	47	710
REP _{AV}	0.335	0.271	1.052	-0.108	0.57	0.207	0.197	-0.064	0.148	-18	43	44
MULTI _{AV}	0.335	0.278	1.184	-0.047	0.50	0.271	0.265	-0.057	0.176	-17	48	44

Table S.8: Statistics associated with satellite Chl computed over the MedBiOp dataset. Satellite Chl is the REP (derived by the application of the MedOC4.2018 to the Rrs derived from the CCIv3 processor) and NRT/DT (derived by the application of the MedOC4.2018 to the Rrs derived from the Multi processing). A subset of matchups on the period (2012 to present) in which VIIRS and MODIS-AQUA co-exist (REP_{AV} and Multi_{AV}) is also reported.

KD490	\bar{X}^M	\bar{X}^E	SLOPE	INTERCEPT	r^2	RMSD	CRMSE	BIAS	MAE	RPD	APD	N
MULTI	0.053	0.072	0.775	-0.165	0.75	0.048	0.044	0.019	0.02	44	47	420
GLOBAL	0.053	0.058	0.857	-0.145	0.83	0.023	0.023	0.005	0.01	15	24	420

Table S.9: Statistics associated with satellite-derived kd490 computed in correspondence of the BGC-Argo float dataset (Organelli et al., 2017), whose location is shown in Figure 10b of the main text. The two rows refer to the satellite-derived Kd490 obtained with the Medkd.2018 and the Global algorithm, respectively, as shown in Figure 5 of the main text.

CHL	SLOPE	INTERCEPT	r^2	RMSD(LOG)	CRMSE(LOG)	BIAS(LOG)	N
REP	0.74	-0.306	0.75	0.25	0.25	-0.0428	710
MULTI	0.75	-0.309	0.74	0.26	0.25	-0.0600	710

Deleted: R2

Deleted: 0999

Deleted: 0905

Deleted: 253

Deleted: 250

Deleted: 043

Deleted: 200

Deleted: 8

Deleted: ULTI

Deleted: 0999

Deleted: 0870

Deleted: 308

Deleted: 259

Deleted: 252

Deleted: 060

Deleted: 207

Deleted: 8

Deleted: 2708

Deleted: 1970

Deleted: 42

Deleted: 198

Deleted: 138

Deleted: 218

Deleted: 2708

Deleted: 1911

Deleted: 3

Deleted: 3

Deleted: 227

Deleted: 151

Deleted: 246

Deleted: 2017

Deleted: R2

Deleted: 6

Deleted: 996

Deleted: 079

Deleted: 826

Deleted: 135

Deleted: 105

Deleted: 86

Deleted: 25

Deleted: 30

CAR	0.72	-0.056	0.76	0.31	0.31	0.0066	14582
------------	-------------	---------------	-------------	-------------	-------------	---------------	--------------

Table S.10: Chl matchup statistics as in Table S.8 for REP and Multi. The difference is that Chl log-transformation is here used to compute all the statistical parameters, not only those associated with the linear fit (Slope, Intercept and determination coefficient). CAR statistics are those of Figure 8 in the Ocean Colour Climate Change Initiative (Phase Two) Climate Assessment Report (http://esa-oceancolour-cci.org/?q=webfm_send/702).

Page 3: [1] Deleted	Gianluca Volpe	11/19/18 4:04:00 PM
Page 4: [2] Deleted	Gianluca Volpe	11/19/18 4:04:00 PM
Page 5: [3] Deleted	Gianluca Volpe	11/19/18 4:10:00 PM
Page 6: [4] Deleted	Gianluca Volpe	11/19/18 4:13:00 PM
Page 7: [5] Deleted	Gianluca Volpe	11/19/18 4:14:00 PM
Page 8: [6] Deleted	Gianluca Volpe	11/19/18 4:15:00 PM
Page 9: [7] Deleted	Gianluca Volpe	11/19/18 4:16:00 PM